Union College
Union | Digital Works

Honors Theses | Student Work

6-2018

High Performance Thermal Insulation: Silica Aerogels in Construction Technology

Matthew Giarrusso

Follow this and additional works at: https://digitalworks.union.edu/theses

 Part of the Heat Transfer, Combustion Commons, Mechanics of Materials Commons, and the Other Engineering Science and Materials Commons

Recommended Citation
Giarrusso, Matthew, "High Performance Thermal Insulation: Silica Aerogels in Construction Technology" (2018). *Honors Theses*. 1646.
https://digitalworks.union.edu/theses/1646

This Open Access is brought to you for free and open access by the Student Work at Union | Digital Works. It has been accepted for inclusion in Honors Theses by an authorized administrator of Union | Digital Works. For more information, please contact digitalworks@union.edu.

Union College Department of Mechanical Engineering

High Performance Thermal Insulation: Silica Aerogels in Construction Technology

By

Matthew Giarrusso

****

Submitted in partial fulfillment

of the requirements for

Honors in the Department of Mechanical Engineering

UNION COLLEGE

May, 2018

Abstract

GIARRUSSO, MATTHEW High Performance Thermal Insulation: Silica Aerogels in Construction Technology. Department of Mechanical Engineering, May 2018

ADVISOR: Professor Ann Anderson

The United States is a world leader in the production and expenditure of energy, accounting for 18% of the total global energy consumption in 2016, 40% of which was used for the heating, cooling, and lighting of commercial and residential buildings. Currently, traditional air-based insulation products are being used in thicker and more numerous layers in an attempt to keep up with contemporary codes and standards. One promising alternative to traditional insulation is silica aerogel. With a remarkably low density and thermal conductivity, silica aerogel could save energy, space, and weight in new and retrofit structures. Silica aerogels are currently most widely used in the construction industry in the form of fibrous blankets containing aerogel. These blankets are typically made using low temperature supercritical drying with CO_2, a process that takes days to complete. Union College uses a patented process known as Rapid Supercritical Extraction (RSCE) where the precursor solution is poured into a mold and subjected to high temperatures and pressure via a hot press to achieve a supercritical state and create an aerogel. This process results in an aerogel in a few hours. The focus of this project was on making aerogel blankets using the RSCE method and comparing them to commercially available products. Specimens were made using both rock wool and quartz felt as the fibrous batting. The thermal conductivity of each sample was measured using the hot disk method and their flammability was quantified by a vertical burn bench test. The thermal conductivity of the commercial, quartz felt, and rock wool blankets were found to be 0.035, 0.037, and 0.046 W/mK respectively, less than or comparable to that of commercial fiberglass insulation (0.045 W/mK). When applied to the exterior of studs in a typical New England home the application of silica aerogel insulation could result in 483 to 855 fewer kilograms of carbon dioxide being released into the atmosphere annually. A mock building was designed, constructed, and outfitted with an aerogel window and insulation to demonstrate the practicality and the energy savings afforded by the use of aerogels in construction. This report will cover the fabrication of an aerogel blanket as well analytical and experimental methods used to quantify the benefits of aerogel insulation.

Table of Contents

List of Figures

List of Tables

Chapter 1 - Introduction

Earths average surface temperature has risen 1.1 ℃ since 1880, with roughly two thirds of this warming occurring since 1975 [1]. Sixteen of the 17 warmest years on record have occurred since 2001 and this trend shows no signs of stopping. The Intergovernmental Panel on Climate Change (IPCC) predicts that in the 21st century the global surface temperature is likely to rise another 1.1-2.9℃ in the best-case scenario or 2.4-6.4℃ worst-case scenario [2]. This poses a very real threat to society as we know it as prolonged periods of raised temperatures have been linked to severe draughts and floods, more acidic oceans, and rising sea levels affecting everyone on earth in some capacity [3]. The IPCC has concluded that this global warming is largely due to increased concentrations of greenhouse gasses produced by humans, primarily through deforestation and the burning of fossil fuels. Figure 1 shows a graph of temperature change versus atmospheric carbon dioxide concentration.

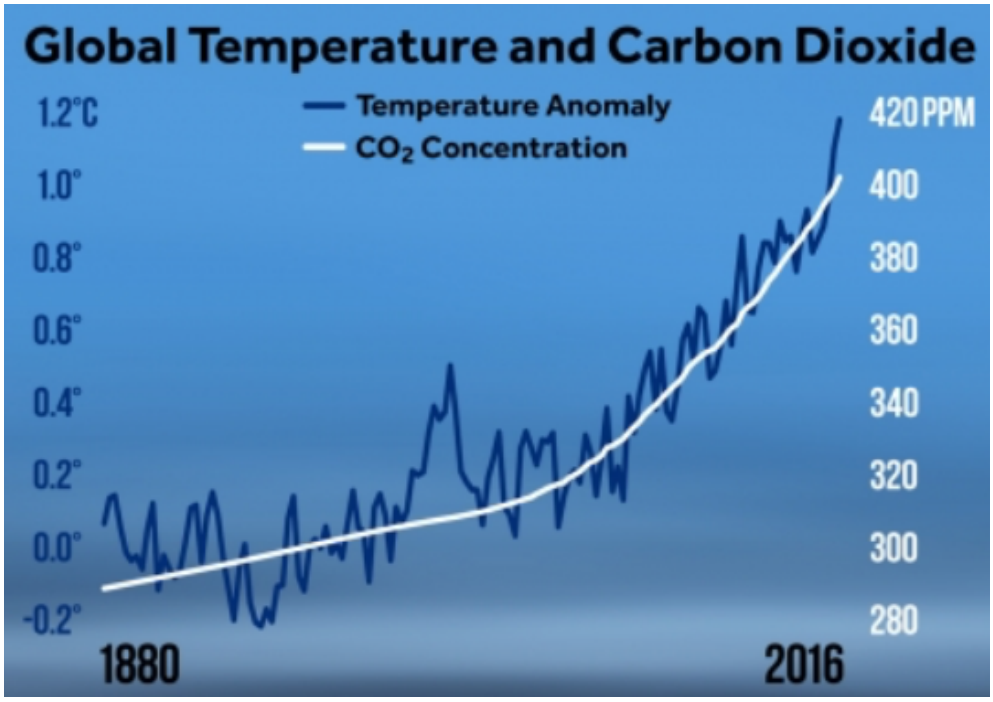

Figure 1 shows carbon dioxide concentration versus temperature rise [4].

In order to diminish the harmful effects of global temperature rise scientists have had to rethink global energy strategies in order to minimize greenhouse gas production. In December of 2015 the Paris Agreement was adopted by the United Nations with the goal of encouraging countries to collaborate to keep global temperature change below 2℃, and has since been signed by 195 nations of the United Nations

Framework Convention on Climate Change. This has resulted in a massive influx of funding into the research and development of renewable energy technologies. While this has had a considerable positive influence on the global production of greenhouse gasses the transition is not happening fast enough to keep us below the 2℃ threshold, with renewable resources supplying only about 19.3% of the total world energy demand [5]. In order to successfully reach the goals laid out by the Paris Agreement vast strides must be made in energy management and efficient energy consumption.

In order to abate the effects of greenhouse gas emissions it is necessary to evaluate consumption levels and their distribution by sector. The United States is a world leader in the production and expenditure of energy, accounting for 18% of the total global energy consumption by using 97.4 quadrillion Btu in 2016 [6]. Of the nearly one thousand million Btu consumed, 40% was used for the heating, cooling, and lighting of commercial and residential buildings as specified in Figure 2 [7].

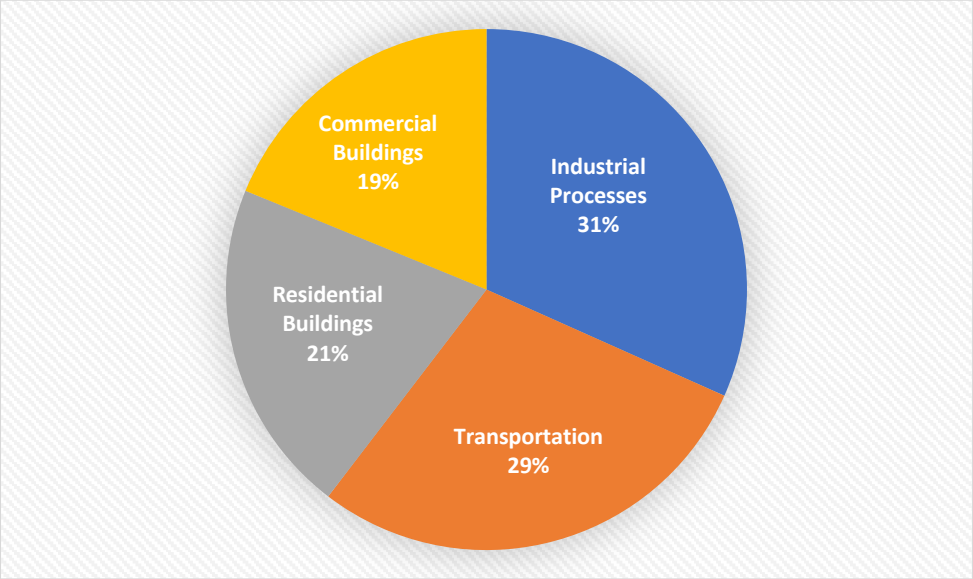

Figure 2 breaks down the share of total US energy used by sector. [7]

The colossal amounts of energy being used to heat and cool buildings makes residential and commercial retrofit insulation one of the easiest, most cost-effective means for decreasing greenhouse gas emissions [8]. Thermal insulation serves as a means to minimize the amount of heat transfer through the envelope of a building in order to curtail the amount of energy required to keep the interior at a desired temperature. Currently traditional air based insulation materials are being used in thicker and more numerous layers in an attempt to meet contemporary codes and standards; consequently, this is leading to heavier and more complex structures, as well as reducing the net-to-gross floor area, or livable space [9].

The heat transfer through insulation material is divided into three main components, convection through the gas, conduction through the solid, and radiation through pores. In conventional insulation materials such as mineral wool and fiberglass the total thermal conductivity, or the materials ability to transfer heat, is dominated by the conductivity of the gas within the medium, typically air. Figure 3 shows the breakdown of conductivity factors as a function of material density and how they influence the total thermal conductivity in conventional insulation materials.

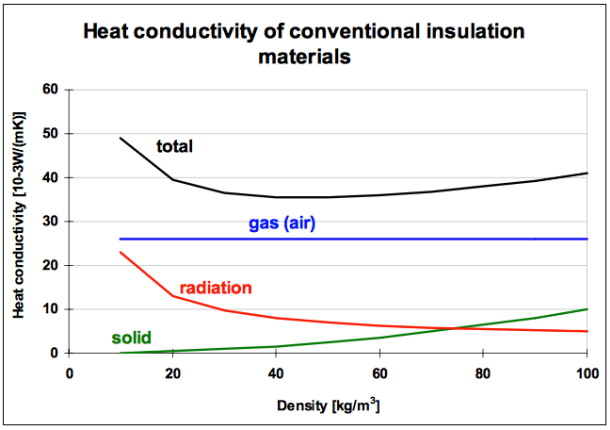

Figure 3 demonstrates heat conductivity of conventional fiber and foam insulation. [10]

A significant amount of building energy efficiency can be gained by reducing the gas conductivity in insulation materials. In a porous substance, the gas conductivity is a function of the amount of gas present in the medium, as well as the number of barriers encountered moving from one side of the material to the other. The addition of "walls" by reducing pore size in the insulation limits collisions between gas particles ergo limiting effective heat transfer.

In this regard silica aerogels are one of the most promising new insulation materials on the market. Aerogels are sol-gel materials that are dried in a manner that prevents pores from collapsing, leaving a material that is 90-99% air by volume. The resulting solid consists of a silica nanostructure with a large number of pores typically between 10 and 100 nm in diameter. The high porosity means that silica aerogel monoliths can be prepared with thermal conductivities (k) and densities (ρ) as low as 0.02 W/mK and 0.05 g/cm^3 respectively [11]. Comparatively, common insulation materials such as mineral wool, glass wool, and polystyrene have thermal conductivity values ranging from 0.03 to 0.04 W/mK [12]. Table 1 displays a variety of common insulation materials and their respective thermal conductivity range.

Table 1 compares aerogel to common insulation material [12].

Insulation Product	***Fire Resistance***	***Durability***	***λ (W/mK)***
Fiberglass Blankets	Good	Compression Reduces R-Value	0.033-0.44
Rockwool Blankets	Excellent	Compression Reduces R-Value	0.037
Polyethylene Blankets	Poor	R-Value Decreases with Time	0.041
Blown in Fiberglass	Good	Comp. and Moisture Reduce R-Value	0.030-0.038
Blown in Rock Wool	Excellent	Comp. and Moisture Reduce R-Value	0.040
Blown in Cellulose (Recycled Paper Products)	Good (With the Addition of Fire Resistant Chemicals)	Comp. and Moisture Reduce R-Value	0.046-0.054
Fiberglass Boards	Good	Rigid	0.032-0.035
Expanded Polystyrene	Poor	Rigid	0.037-0.038
Extruded Polystyrene	Poor	Rigid	0.030-0.032
Solid Aerogel	Excellent	Rigid	0.012-0.020
Aerogel Blanket(Silica)	Excellent	Excellent	0.015 [13]

Silica aerogels are typically made using a two-step process. First, a silica source such as tetramethylorthosilicate (TMOS) is mixed with deionized water, methanol, and ammonium hydroxide in a prescribed molar ratio creating a wet-gel in a sol-gel polymerization reaction. The gel consists of a porous SiO_2 solid matrix where the pores are filled with methanol and water, the byproducts of the polycondensation reaction. The gel is then dried, removing the solvent without altering the matrix. This is typically done via supercritical extraction, freeze drying, or ambient-pressure drying [14]. Union College uses a patented Rapid Supercritical Extraction (RSCE) process allowing monolithic aerogels to be fabricated in a matter of hours rather than the days or weeks needed by other methods. Accelerated production of aerogels could reduce prices and encourage widespread adoption of aerogel technology in the construction realm.

One of the primary methods of heat loss in a building is through thermal bridging. Thermal bridging occurs when a more conductive material provides an easy pathway for heat transfer through an otherwise sound thermal barrier. The most egregious offender is a necessary structural component: wood and metal studs. Figure 4 shows an infrared image of a typical New England home. The green vertical lines and yellow

surrounding the windows are indicative of higher heat transfer through the wood studs, decreasing the efficiency of a conventionally insulated building envelope.

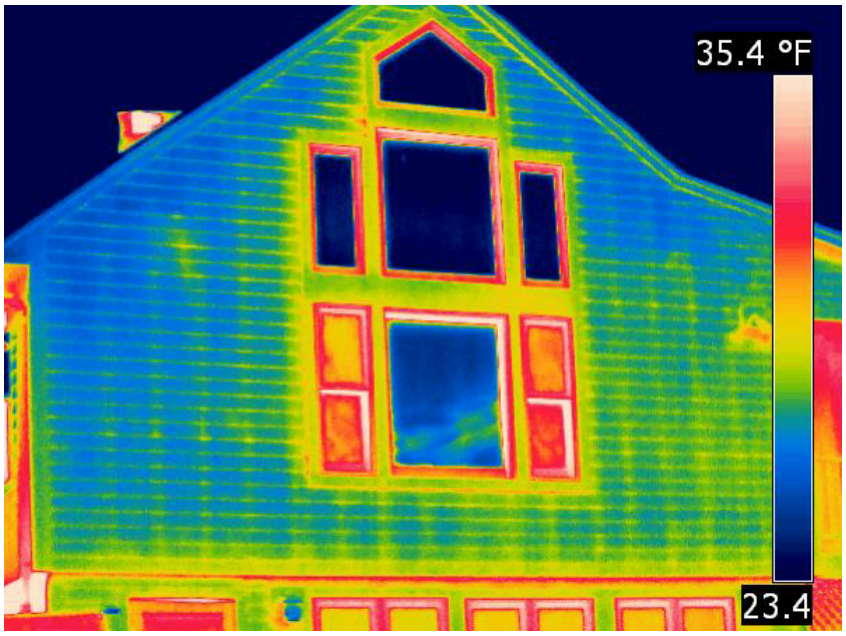

Figure 4 shows thermal bridging in a typical residential building. [15]

Jan Kosney [16] explored the effects of aerogel strips on the total thermal resistance (R-value) of building envelopes. Kosney concluded that the addition of ¼ inch thick by 2.5-inch-wide aerogel strips to the exterior of studs could increase the total R-value of a wood framed building envelope by 9%. The application of the same ¼ inch thick by 2.5-inch-wide aerogel strips to the exterior of steel studs increased the total R-value of a steel framed building envelope by nearly 29% as tested in a guarded hot box. Based on these results aerogel strips present a good potential for the thermal improvement of building envelopes provided their cost can be driven down.

Aspen Aerogels and the Cabot Corporation are two of the leading manufacturers of aerogel products. They offer a variety of goods ranging from aerogel particles for daylighting architectural use to aerogel wraps for subsea pipelines and aerospace fire protection. While aerogels fill many niche applications the most widespread products are insulating aerogel blankets for use as space saving insulation in residential and commercial buildings. These aerogel products are made in bulk via low temperature supercritical drying with CO_2.

The purpose of this project is to evaluate if silica aerogel blankets can be fabricated using the Union College RSCE process and evaluate how these aerogel blankets compare to analogous aerogel blankets already on the market. The aerogel blankets will be produced using either quartz felt or rock wool set in aerogel in different quantities and orientations in order to improve the material strength of the aerogel composite. If a viable aerogel blanket is produced it will be tested against comparable aerogel blankets already on the market to ensure it retains its thermal performance and meets flammability standards imposed on building materials. Furthermore, a scaled down mock building will be produced containing aerogel windows and insulation. A heating element will be added to the interior of the building to simulate typical conditions. Thermal images will be captured to help emphasize the positive effects of aerogel windows and insulation.

If silica aerogel blankets can be produced at a competitive cost and a rapid rate they can be part of the solution to a global problem of climate change and energy efficiency. While they are not a definitive solution, by retrofitting older, inefficient buildings and ensuring that new construction meets rigorous energy efficiency requirements we can continue to abate the emission of harmful greenhouse gasses while gaining back valuable living space. In conjunction with an uncompromising pursuit of renewable energy sources, new superinsulations such as silica aerogels can help hit the goals set forth by the 2015 Paris Accord and diminish or avert some of the harmful effects of global temperature rise.

The following chapter outlines the process for fabricating an aerogel using the Union College RSCE process. The subsequent two chapters discuss methods for determining the thermal conductivity and flammability of the resulting blanket respectively. The final chapter discusses the design for the mock building using aerogel products as well as the means by which heat transfer through the building envelope will be determined.

Chapter 2 - Fabricating an Aerogel Blanket

2.1: Materials

Aerogel blankets are composed of a lofty batting which is impregnated by aerogel. The lofty batting is a fibrous material which minimizes the amount of unsupported aerogel while maintaining or only marginally diminishing the thermal performance of the aerogel. Some suitable fibrous materials include fiberglass, polyester, Kevlar, and carbon fibers. For the preparation of these samples quartz felt and rock wool were chosen. Quartz felt is fused quartz wool which has been impregnated with a starch binder to provide a stable sheet which can easily be cut to exact sizes. A 0.5 x 0.5-meter quartz felt mat was purchased from Technical Glass Products for use in this project. Lab grade rock wool was left over from a prior student's work. Both options provide the necessary structural integrity and flexibility to the aerogel composite without significantly disturbing the thermal properties of the aerogel due to their extremely low thermal conductivities, typically 0.04 W/mK at 25℃. Furthermore, each is able to withstand the high pressure and temperatures imposed upon the samples by the RSCE method without appreciably deteriorating.

The mold was constructed of 6 x 6 x 0.5-inch 4140 alloy steel purchased from McMaster-Carr. The mold was finished in the Union College machine shop and includes two 5 x 1.5-inch bays. The bays are closed bottom to facilitate an easier sealing process and are 5mm deep so as to be easily compared to the 5mm thick Aspen Spaceloft product. Figure 5 shows the mold used to fabricate the aerogel blankets. Detailed drawings of the mold can be found in Appendix A.

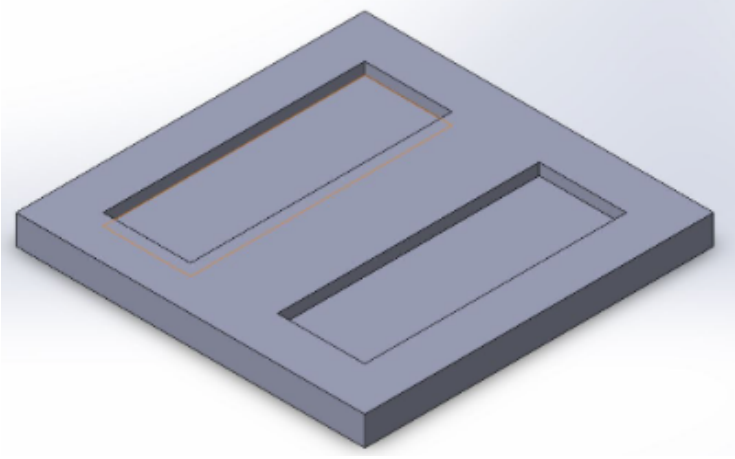

Figure 5 shows the mold which creates 2 aerogel blanket strips.

The aerogel precursor solution contains Tetramethylorthosilicate (TMOS), deionized water, methanol, and ammonium hydroxide in a prescribed molar ratio resulting in a wet-gel. Typical quantities for each can be found in Table 2. TMOS reacts with deionized was and provides the silica for the nanosctructure. Methanol is miscible with TMOS as well as deionized water, ensuring that they remain in the same phase so a reaction may occur. Ammonium hydroxide acts as a catalyst to the reaction. Specific chemical ratios for each sample created can be found in Appendix B.

Table 2 gives typical quantities of the chemicals used to create a wet-gel.

Amount Desired	**100 mL**
TMOS	21.49 mL
Methanol	69.09 mL
Water	8.70 mL
1.5 M Ammonia	716.48 μL

Sealing gaskets are cut from graphite and either aluminum sheet or stainless-steel foil. The 1/16-inch thick graphite gasket material was purchased from Phelps. The stainless-steel foil was 0.0005-inch thick 302/304 stainless steel purchased from Brown Metals. The aluminum was 0.003-inch thick hardened easy-to-form 1100 aluminum sheet purchased from McMaster-Carr.

2.2: Equipment

A programmable hot press was used to apply specified temperatures and pressures for prescribed period of time allowing the gel to form, age, and eventually reach supercritical temperatures and pressures. The hot press used was the Tetrahedron MTP 14 which has a maximum force of 30 tons and can be seen in Figure 6 shows the Union College hot press (photo curtsey of Kian Cook). Typical parameters used in the formation of an aerogel blanket can be found in Table 3; specific parameters used for each sample can be found in Appendix B.

Figure 6 shows the Union College hot press (photo curtsey of Kian Cook)

Table 3 gives typical hot press parameters used in the formation of a silica aerogel blanket.

Step	Temp. (F)	Rate (F/min)	Force (kips)	Rate (kips/min)	Time
1	90	200	45	600	30
2	550	3	45	600	55
3	550	200	1	1	15
4	90	4	1	1	15

2.3: Procedure

TMOS was mixed with deionized water, methanol, and ammonium hydroxide in predetermined amounts. The resulting solution was then sonicated for 5 minutes to ensure it was monophasic. Either quartz felt or rock wool was cut into 5 x 1.5-inch strips and placed into the bays of the mold; special care was taken to ensure no strands protruded from the recess. The solution was poured over the batting and sealing gaskets were cut and placed over the open face of the mold to prevent any chemicals from leaking during the process. Figure 7 shows a prepared sample with and without the gasket material.

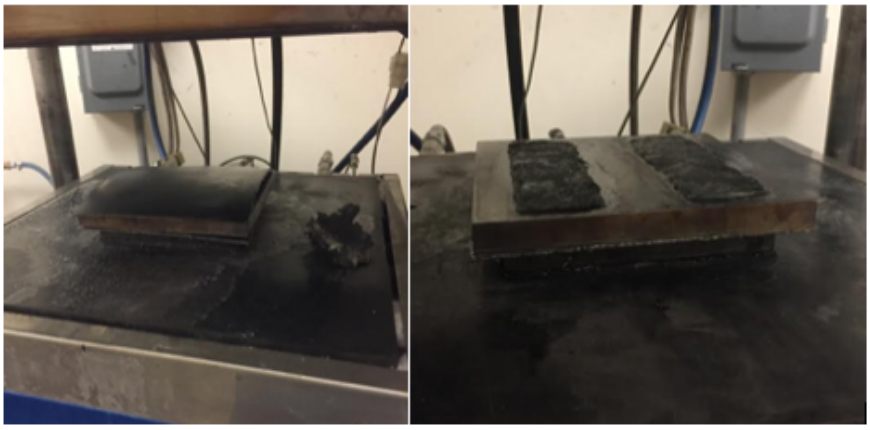

Figure 7 exhibits a quartz felt sample in the mold with (left) and without (right) gasketing.

The mold is then placed between the plates of the hydraulic hot press which applies a great deal of force, sealing the mold and performing the extraction process. At the end of the program the gasket material is removed revealing a completed aerogel blanket.

2.4: Results

Upon removing the gasket material the resulting aerogel blanket is exposed and can be removed from the mold as seen in Figure 8.

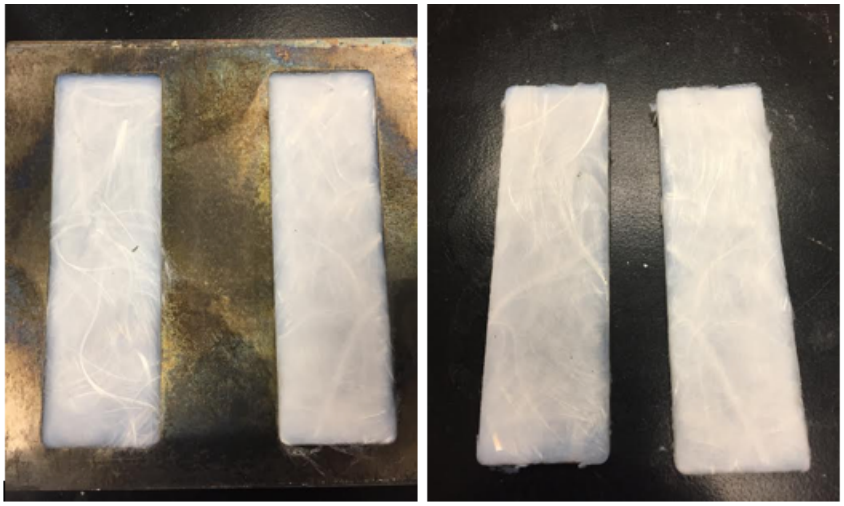

Figure 8 shows the completed rock wool aerogel blanket in (left) and out (right) of the mold.

Analysis of the manner in which the aerogel and the fibrous material bonded was conducted. Although similar in appearance, samples of both the Union College rock wool aerogel blanket and Aspen's

spaceloft were viewed under a Ziess EVO50 scanning electron microscope with the generous help of Tommy Andre as seen in Figure 9.

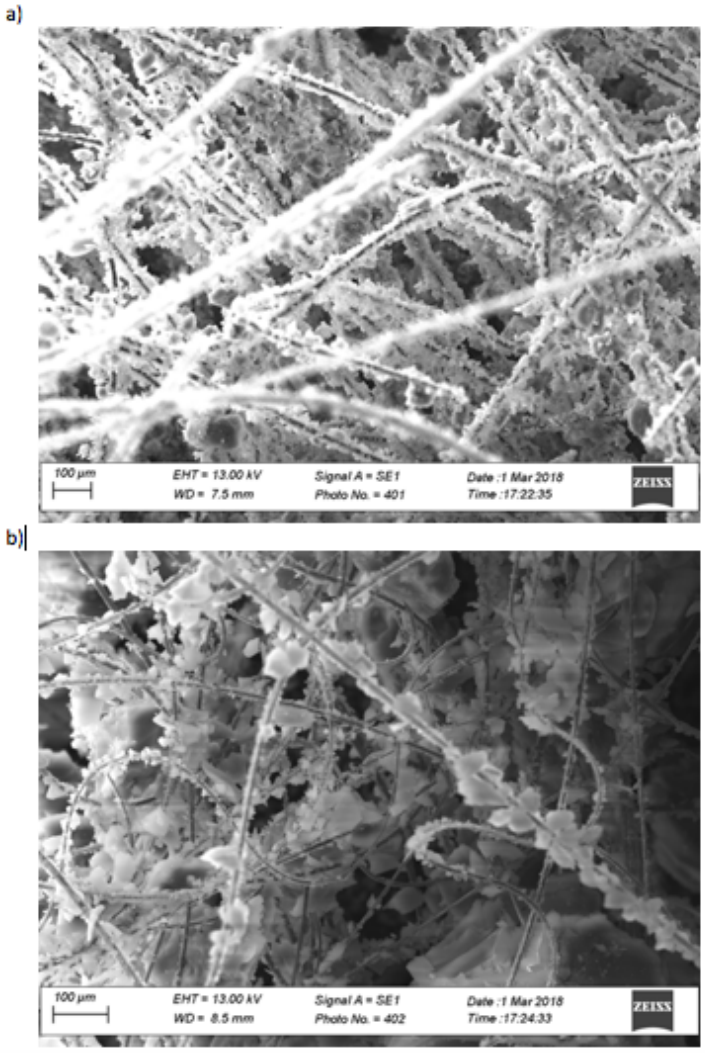

Figure 9 exhibits SEM images of Aspen's Spaceloft (a) and the rock wool aerogel blanket (b).

In each case the images clearly show aerogel granules bound to the long fibers of the lofty batting. While Aspen's spaceloft exhibits more fiber density as well as a more even distribution of aerogel bound to each strand the two samples are very similar in nature indicating the successful fabrication of an aerogel blanket using the RSCE method.

In total six batches of blankets were produced, resulting in twelve samples. Four of the samples consisted of varying amount of rock wool batting, the remaining eight samples contained quartz felt. The

percent composition of each sample was determined using equation 1 where M_{sample} is the mass of the final blanket and $M_{batting}$ is the initial mass of the fibrous batting. Table 4 summarizes the percent content of each sample. The mass of the fibrous batting was unknown for spaceloft and samples 1-1 and 1-2. A complete breakdown of the contents of each sample and hot press parameters used to create them can be found in Appendix B. The following chapters present thermal conductivity and flammability test results as well as analytical and experimental evaluations of the effect of aerogel insulation on heat transfer through a building envelope.

$$\% \text{ content of aerogel by mass} = \frac{M_{sample} - M_{batting}}{M_{sample}} * 100 \quad (1)$$

Table 4 gives the percent content of aerogel by mass for each sample.

Sample Number	**% Aerogel**
Spaceloft	(?)
1-1	(?)
1-2	(?)
2-1	81.26
2-2	88.66
3-1	85.97
3-2	82.10
4-1	91.51
4-2	88.97
5-1	85.22
5-2	84.71
6-1	51.25
6-1	55.06

Chapter 3 – Thermal Conductivity

3.1: Current Standards

There are several tests that can be useful in measuring the thermal properties of construction materials. These tests are often specific to the size or geometry of the material and typically use a temperature gradient and heat flux through the specimen to extrapolate its thermal properties. The American Society for Testing and Materials (ASTM) dictates technical standards for the testing and classification of a wide range of materials, systems, and services. ASTM standards are widely used to define construction specifications and many companies as well as federal, state, and municipal governments reference them when designating building codes and regulations.

The ASTM sets forth a wide variety of procedures for the testing of insulation and building materials. ASTM C1363-11 describes the standard test method for thermal performance of building materials and envelope assemblies. This method calls for the use of a hot box apparatus which consists of two boxes maintained at specified temperatures surrounded by "guard boxes" of the same temperature to prevent heat loss to the ambient. A schematic of the hot box test is shown in Figure 10.

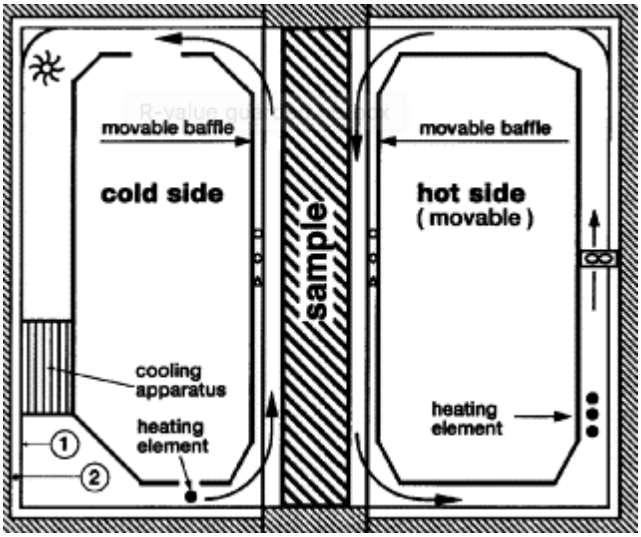

Figure 10 shows a schematic of a hot box apparatus [17].

Using the overall heat added and removed from the system in addition to all potential inadvertent heat losses the R value of the specimen can be calculated. The hot box apparatus is generally a means by which to test large, nonhomogeneous samples for their thermal resistance. This test method can be applied to building structures or composite assemblies and is intended for use at conditions similar to those

experienced by a normal building. While beneficial in measuring the R value of large building elements it is space and cost prohibitive, and reports uncertainties of up to 10%.

Another method that is useful in determining the thermal properties of construction materials is ASTM C177-13: the standard test method for steady state heat flux measurements and thermal transmission properties by means of the guarded hot plate apparatus. This test method is specifically prescribed for the measurement of the thermal conductivity of thin, flat specimens with a low thermal conductivity that are homogenous in the direction of heat transfer. The guarded hot plate method is able to measure the thermal conductivity of insulating materials at steady state with an uncertainty below 2% over a temperature range near ambient when performed properly [18]. The test begins with the specimen being installed in between a heating and a cooling plate made of extremely conductive material to ensure a constant surface temperature across each. The sample, heating, and cooling plates are surrounded by insulation in order to simulate one dimensional heat transfer and prevent the loss of heat to the environment. The test can be either one sided or two sided; Figure 11 shows both types of guarded hot plate tests.

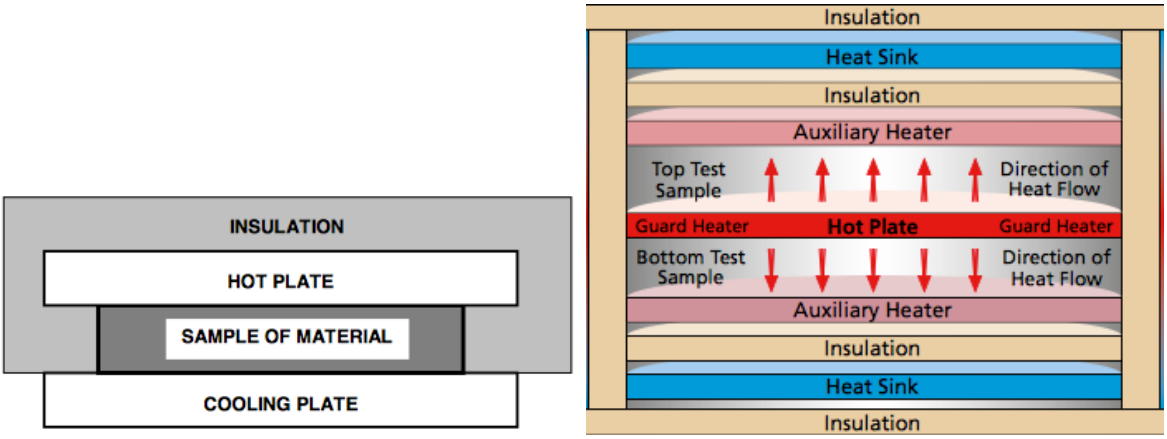

Figure 11 displays (left) a one sided guarded hot plate test and (right) [18] a two-sided guarded hot plate test [19].

The hot and cold plates are heated to pre-determined temperatures and let sit until they are sure to have come to steady state. Knowing the power input into the hot plate (Q), the thickness of the sample (t), and the temperature difference between the hot and cold plates (ΔT) equation 2 can be used to find the thermal conductivity (k) of the sample of interest.

$$k = \frac{Q*t}{\Delta T} \tag{2}$$

3.2: Test Methods

For reasons of availability and convenience, a hot disk was used to measure the thermal conductivity of the aerogel blanket samples. The hot disk uses transient plane source method for measuring thermal conductivity and is approved as an International Organization of Standardization (ISO) method. The hot disk system consists of five individual components as pictured in Figure 12 as well as a computer to record and display the data.

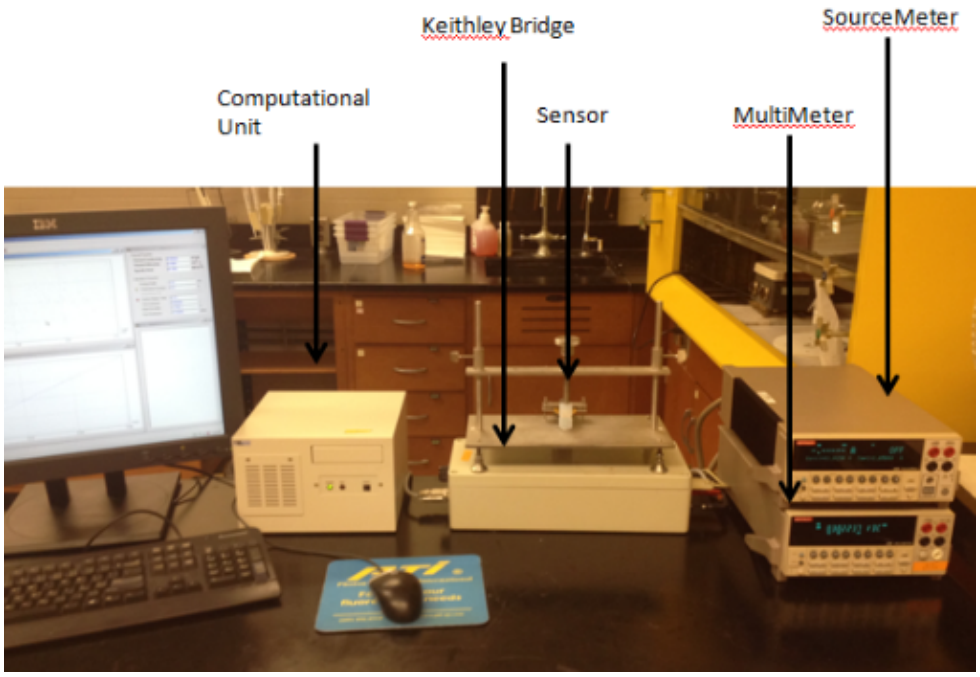

Figure 12 shows the hot disk thermal analyzer system [20].

A flat foil sensor is connected to the Keithley bridge and sandwiched between two halves of the sample to be measured with the diameter of the two halves equaling at least twice that of the sensor. For these purposes the Kapton C5465 sensor was adequate. Figure 13 shows the sensor experimental setup.

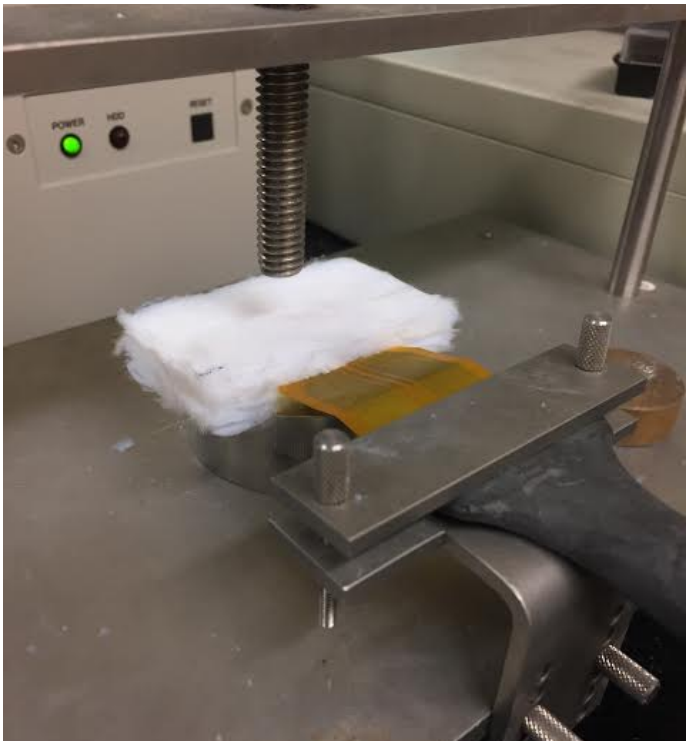

Figure 13 shows the sensor sandwiched between two samples of aerogel blanket sample.

A prescribed current is passed through the sensor spiral for a set amount of time, increasing the temperature of the sensor. As aerogels are highly insulating, a significant amount of heat may build up on the sensor causing it to burn out if a high Wattage is applied. A general rule of thumb in order to minimize error and uncertainty is higher powers for shorter times or lower powers for longer times. For these two reasons a low power of 0.02-0.05 Watts applied for 50 to 110 seconds was chosen for each of the samples analyzed. The parameters used for each sample can be found in Appendix B. The heat generated dissipates from the sensor into the sample at a rate that is contingent upon the thermal properties of the specimen. Using the temperature of the sensor in conjunction with the time elapsed the thermal conductivity and diffusivity of the sample can be calculated to within 5% and 10% accuracy respectively provided the proper parameters are chosen and the experiment is executed with care [21].

3.3: Results

A total of five thermal conductivity measurements were recorded at varying locations on each sample, one through twelve. Additionally, five data points were collected for a sample of Spaceloft as a control. The total thermal conductivity results for the Spaceloft control can be found in Appendix C. To ensure the validity of the results conductivities were only recorded if their Temperature Drift vs Time and

Different Temperature vs square root Time plots were considered sufficiently random. Trends in these plots could indicate the effects of outside phenomena such as temperature irregularities in the sample or errors in the curve fitting process effectively skewing the results. Finally, a temperature rise and total characteristic time of 6-10℃ and 0.3-1.0 respectively are indicative of sufficient power output and experimental time parameters. If a run met the above criterion the measured conductivity was considered credible. If it failed to meet any of the above specifications the sample was allowed to cool before being ran again. After five runs were recorded for each specimen as well as the spaceloft sample the conductivities were averaged and graphed according to their conductivities and composition in Figure 14 below. Additionally, the grand averages for each sample type can be found in Table 5. The complete results of the thermal conductivity tests can also be found in Appendix B.

Table 5 displays the grand averages for each sample type.

	Spaceloft	**Rock Wool**	**Quartz Felt**
Thermal Conductivity [W/(mK)]	0.0355	0.0499	0.0332
Composition Aerogel [%]	(?)	53.0	86.1

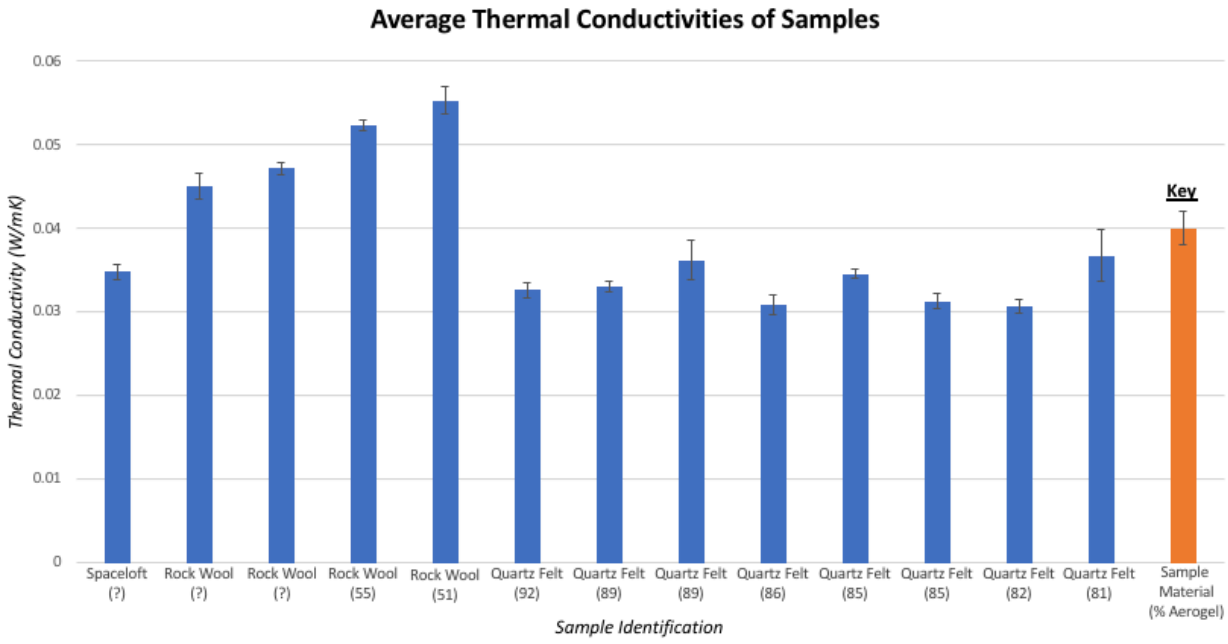

Figure 14 shows the average thermal conductivity of each of the samples.

The rock wool blankets, on average, exhibited a thermal conductivity 43.4% higher than the spaceloft blanket. Furthermore, the rock wool blankets displayed an average thermal conductivity 50.3%

higher than that of the quartz felt blanket and a percent composition by mass of aerogel that was 38.5% lower than the quartz felt samples. This indicates that as the percent content of aerogel increased, the thermal conductivity of the resulting sample decreased. Both rock wool and quartz felt alone have thermal conductivities higher than that of silica aerogel, typically around 0.04-0.045 W/mK at 25℃ [12]. As such it is to be expected that the resultant, aerogel blanket thermal conductivity will decrease with a decrease in fiber and an increase in percent aerogel.

While this trend between the grand averages of the three sample types is noteworthy, it becomes less apparent when comparing the average thermal conductivities of each of the individual samples. There is a fair amount of potential for error involved in the testing of each sample. The samples are non-homogenous, with the fibers distributed haphazardly throughout the blanket. This results in a large degree of variation between conductivity measurements, which are dependent on sensor placement and the surface composition of the specimen. Combined with a maximum of 4% and 11% change in rock wool and quartz felt blanket aerogel content respectively, the anticipated correlation was likely lost to error and random variations in the samples.

Chapter 4 – Flammability

4.1: Current Standards

Building materials and products are carefully regulated in order to mitigate the hazards associated with their flammability and ensure the safety of the occupants. In the United States the National Fire Protection Association (NFPA) is the governing body that dictates fire and building safety codes and standards. The NFPA draws many of its provisions from the International Building Code. Two main sets of requirements must be met when considering a material for construction purposes; the combustibility of the material and the flame spread of the material.

A material is classified as combustible or non-combustible based on ASTM standard E136. ASTM E136 calls for test specimens to be conditioned in an oven at 60℃ for 24 hours. After heat treatment one thermocouple is place in the center of the sample and another is placed on the outside and the sample is placed in a vertical furnace and subjected to 750℃ temperature for 30 minutes. In order to be considered non-combustible 3 of 4 tested specimens must experience weight loss of less than 50% of its initial weight, temperature increase at the thermocouples of less than 30℃, and the specimen cannot visibly flame [22]. Alternative test methods such as NFPA 259, the test for potential heat of building materials, have been developed for materials of low combustibility but are not required by current building codes. Extensive testing has been done on the thermal properties of aerogels and they are considered a non-flammable material [23]. Likewise, the Aspen Aerogels product sheet lists aerogel blankets as non-flammable, for this reason this report will not explore the combustibility of aerogel blankets.

The surface burning characteristics of buildings materials are characterized by ASTM E84, which quantizes surface flame and smoke development. The burning behavior of the material is determined by the flame spread index (FSI), the rate a flame will spread over the surface, and the smoke developed index (SDI), which measures the amount and density of smoke emitted from the material. The FSI and SDI are non-dimensional, relative statistics in which asbestos concrete has a value of 0 and red oak wood has a value of 100. ASTM E84 dictates three classes of building materials; Class A is the most fire-resistant consisting of mostly inorganic materials and requiring an FSI of 25 or less, Class B which requires an FSI between 26 and 75, and Class C which an FSI from 76 to 200. All three classes require an SDI of 450 or less. While ASTM E84 is the approved method for determining the flame propagation and smoke production of building materials it requires a 24-foot-long Steiner tunnel, pictured in Figure 15, which is not readily available at Union College. The materials are placed within the tunnel and a flame is applied, the flame spread is observed visibly and the SDI is recorded as a function of optical smoke density.

Figure 15 presents a Steiner tunnel used for the testing of building materials [24].

Many of the current methods of testing flammability are not viable due to size, convenience, or price. Furthermore, the ASTM prescribed standards classify materials as either flammable or non-flammable but many materials, such as aerogel blankets, do not ignite which allows them to automatically pass the test without further considering how the material performs when exposed to heat.

4.2: Test Methods

For the purpose of this experiment the UL94 vertical burn test will be used. This test takes into account more variables and is beneficial in classifying materials that do not ignite. A 0.5 x 5-inch specimen is held vertically in a clamp with the end of the specimen 12 inches from the bench. Figure 16 shows the test configuration for the vertical burn test.

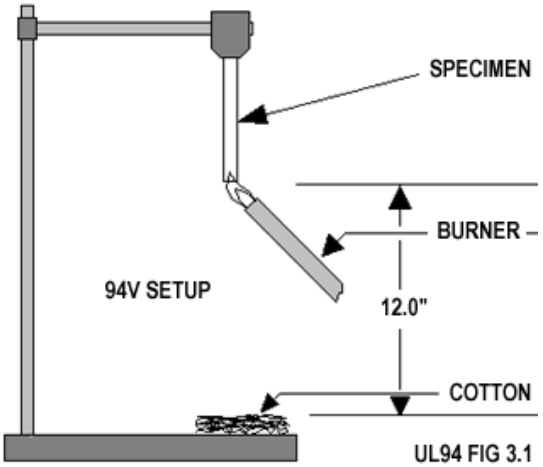

Figure 16 shows the test configuration for a UL94 vertical burn test [25].

A burner flame is applied to the free end of the specimen for ten seconds, the flame is removed until flaming combustion ceases and the flame is re-applied for another 10 second interval. Five specimens are tested and classified via the duration of flaming combustion after the first and second flame applications, the duration of glowing combustion after the second application, whether drips ignite cotton placed below the specimen, the char length, and whether or not the specimen burns to the holding clamp. Table 6 describes the parameters used to compare the Union College aerogel blanket to the Aspen Spaceloft blanket.

Table 6 displays the properties used to characterize the samples.

Criteria
Total Flaming Combustion Time – first burn
Total Flaming Combustion Time – second burn
Glowing Combustion Time after second burn
Cotton Ignited by Drips?
Char length
Does it burn to the holder?

The UL-94 test classifies materials into three different categories. V-0 is the most flame retardant, followed by V-2 and finally V-3 which is the most flammable. The exact criteria used to classify materials is found in Table 7.

Table 7 exhibits the criteria used to classify materials in the UL-95 burn test.

	V-0	**V-1**	**V-2**
Combustion 1 (s)	<10	<30	<30
Combustion 2 (s)	<10	<50	<50
Glowing 2 (s)	<30	<60	<60
Cotton Ignited?	No	No	Yes
Char length (mm)	-----	-----	-----
Burn to Holder?	No	No	No

4.3: Results

A total of six burn tests were performed; two tests for each of the three sample types. Each 1.5 x 5-inch specimen was clamped 12 inches from the bench in a fume hood with cotton balls spread beneath the sample. A propane torch was ignited and applied vertically to the free end for two, ten-second intervals. A stopwatch was used to time the first and second flaming combustion times as well as the glowing combustion time. The experimental setup can be seen in Figure 17.

Figure 17 shows the experimental setup for the UL-94 vertical burn test.

After the culmination of the second, ten-second interval the torch was shut off and the hood closed in order to prevent wind or other environmental anomalies from affecting the results. After the successful completion of a run the sample was removed from the clamp and a ruler was used to measure the char length. The results are displayed in Table 8.

Table 8 presents the results of the UL-94 vertical burn test.

	Spaceloft 1	**Spaceloft 2**	**Quartz 1**	**Quartz 2**	**Rock 1**	**Rock 2**
Combustion 1 (s)	3.79	5.7	0	0	0	0
Combustion 2 (s)	1.42	2.13	0	0	0	0
Glowing 2 (s)	3.76	6.35	1.36	1.9	4	5.83
Cotton Ignited?	No	No	No	No	No	No
Char length (mm)	85.0	93.0	0	0	0	0
Burn to Holder?	No	No	No	No	No	No

While each of the samples meets the criterion to be classified at a V-0, or non-flammable the spaceloft samples performed worse than both the quartz felt and the rock wool samples. In particular the spaceloft exhibited significantly larger combustion times and char lengths. Figure 18 displays the remnants of the samples following the burn test.

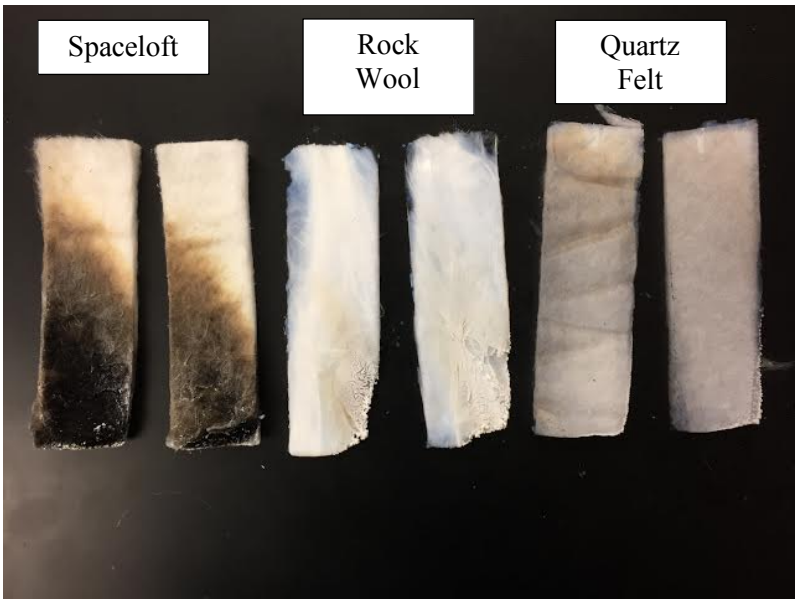

Figure 18 shows samples that underwent the UL-94 burn test.

The spaceloft samples are the only to exhibit clear charring, running nearly the length of the sample. While the rock wool samples show signs of melting along the right-hand side they failed to combust or ignite the cotton reducing cause for concern. The quartz felt samples performed the best, giving little to no indication that they underwent the flammability test.

Chapter 5 – Model Home

While bench tests are useful in determining the thermal conductivity and flammability of an aerogel blanket they do not necessarily correlate to widespread use in the construction industry. Aerogels are currently used in niche applications, but they do not enjoy a large market presence. In order to study the practical applications of aerogels in the construction realm the benefits must be clearly quantifiable and present undeniable benefits which outweigh the costs. The following sections analyze the heat transfer through a scaled down building envelope with and without aerogel products in order to appraise the energy savings afforded by aerogel insulation and windows. First, a conceptual design for a scaled down home was created. A one-dimensional heat transfer model was then devised to approximate the theoretical heat transfer through an aerogel insulated wall versus a conventionally insulated wall. Then, a Solidworks 3D numerical heat transfer model was created in order to reaffirm the 1D results as well as help finalize any design decisions. Finally, the scaled down, mock building envelope was constructed in order to tangibly demonstrate the benefits of outfitting a home with aerogel products. For the sake of the following models the temperature difference between the interior and exterior, ΔT, is assumed to be 70 K. Figure 19 shows the initial concept drawings as created in Solidworks.

Figure 19 shows the initial concept drawings of the mock house.

5.1: Design

A scaled down, mock building was designed to effectively demonstrate the benefits of outfitting a home with aerogel products within the confines of the lab space. The foundation of the model home was

planned to measure 24 x 25-inches with the walls being 18 inches tall and the roof coming to a peak at a height of 31.5 inches. Two opposing walls were to contain 6.5 x 6.5-inch holes into which one aerogel and one conventional window provided by Kian Cook (ME ’18) were designed to fit, the remaining two walls were to be unbroken. Figure 20 provides dimensions of the mock up.

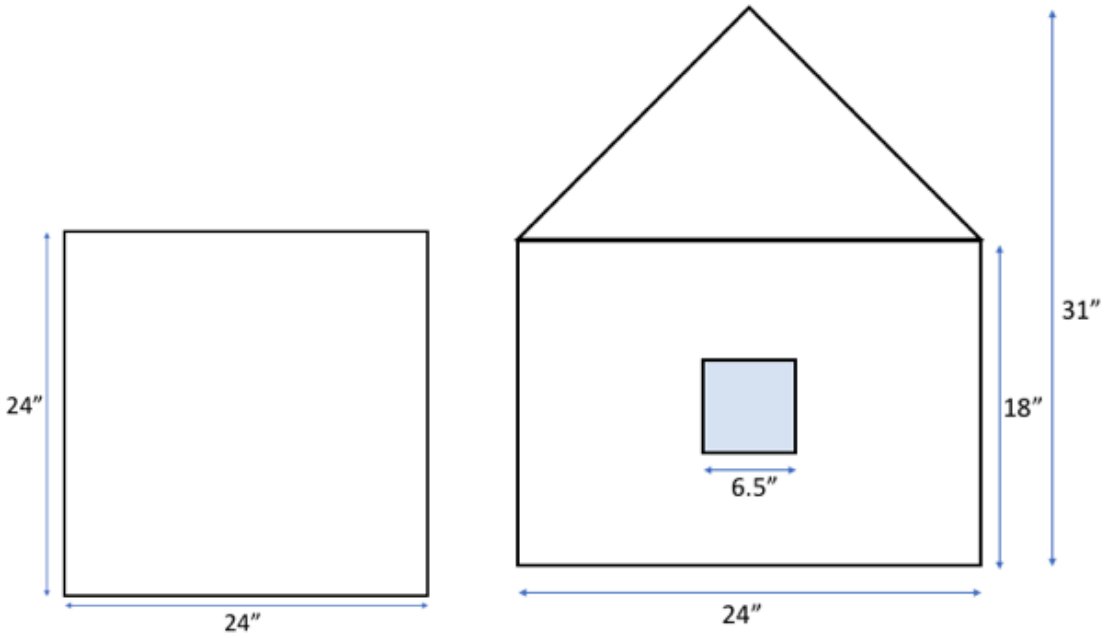

Figure 20 shows the floor plan of the mock up (left) and the elevation plan of the front of the mock building (right)

The mock up was to use 2x4 wood framed walls clad in ½ inch thick plywood sheathing modeling the construction of a conventional residential home. The roof was planned to be clad in asphalt shingles. The walls and roof of the house were to be insulated with fiberglass insulation batts with an R value of at least 13 m^2K/W and the roof will be insulated with R- 38 as recommended by the department of energy [26]. The exterior of the studs of two of the four walls were to be outfitted with 5 mm thick aerogel strips to reduce thermal bridging. Figure 21 shows a cross section of an aerogel wall assembly at a stud without a window.

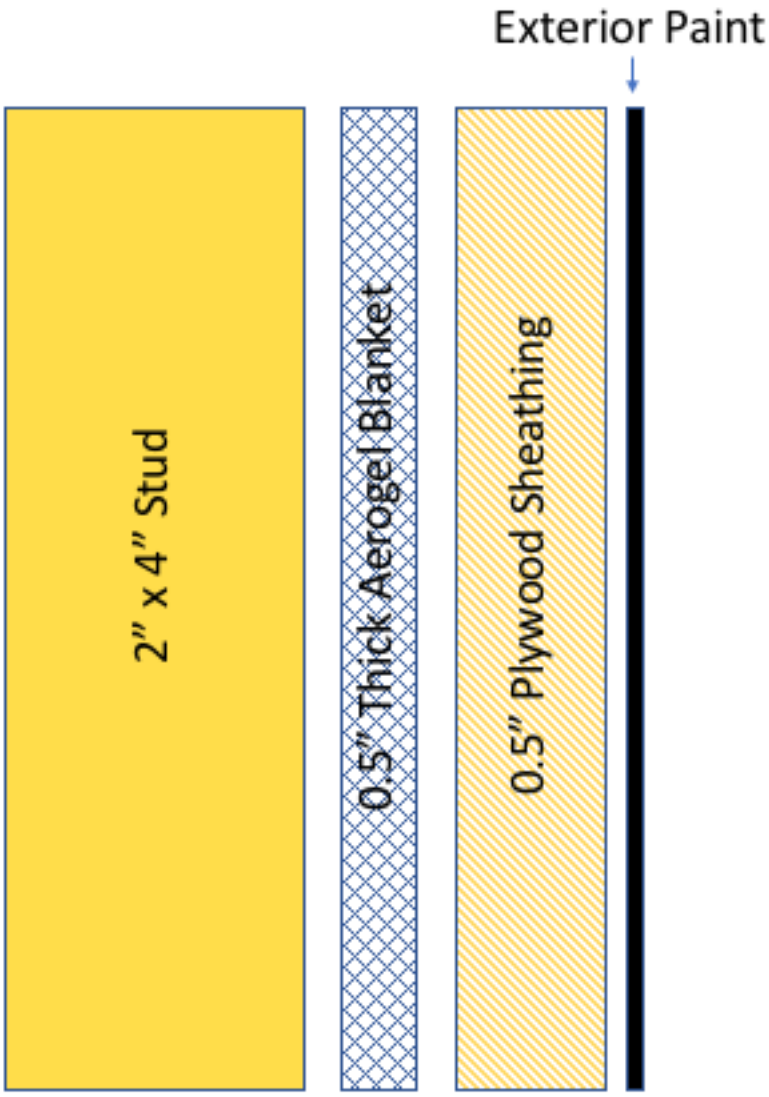

Figure 21 shows a cross section of a portion of the wall over a stud.

While this design is a good approximation of the envelope of a house there are some limiting factors. The design does not include trim around the windows, interior finishes such as drywall, exterior finishes such as siding, or heating or ventilation systems.

5.2: One Dimensional Heat Transfer Model

Prior to construction, a 1D heat transfer model was crafted in order to predict the difference in heat loss between a building with and without aerogel insulation. To simplify the model a single wall with a window was evaluated with and without aerogel features. Figure 22 shows the design of the wall analyzed.

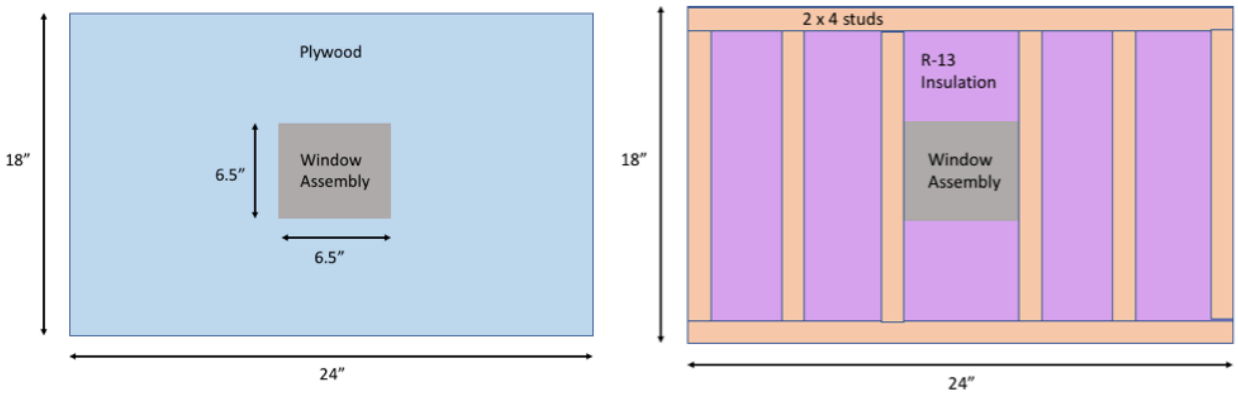

Figure 22 displays the inside (left) and outside (right) of the wall design used for the mathematical model.

To determine the heat transfer rate, q_x, the wall is assumed to be a plane wall undergoing one dimensional heat transfer. As such the heat transfer rate can be described according to equation 3 where ΔT is the overall temperature difference and R_{tot} is the total thermal resistance of the envelope.

$$q_x = \frac{\Delta T}{R_{tot}} \tag{3}$$

Knowing ΔT, thermal resistance diagrams were created to determine the equivalent resistance of the entire wall structure. The thermal resistance diagrams for the walls with and without aerogel insulation are shown in Figure 23 and Figure 24 respectively. The top branch of each resistance diagram represents flow through the window assembly, the middle branch is flow through a stud to the exterior and the bottom branch represents a path through the insulated area between studs.

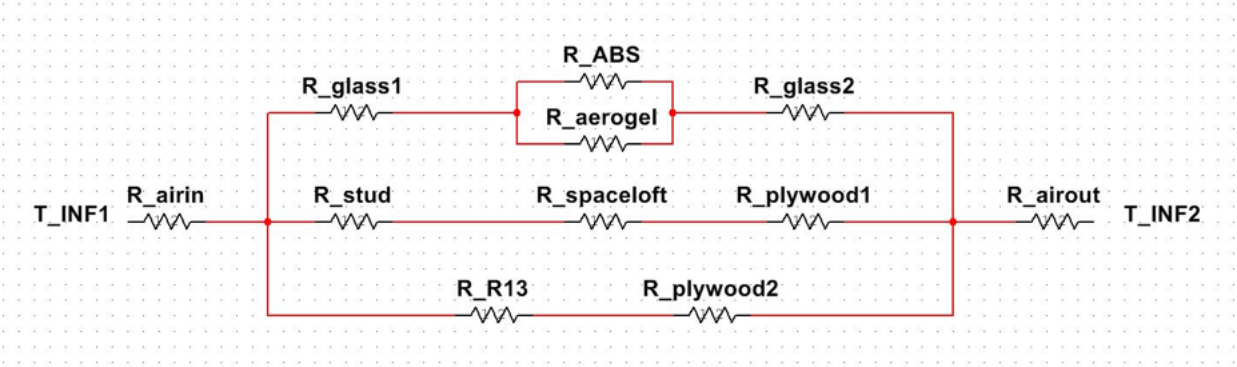

Figure 23 shows the resistance diagram for the aerogel wall (Curtesy of Kian Cook ME '18).

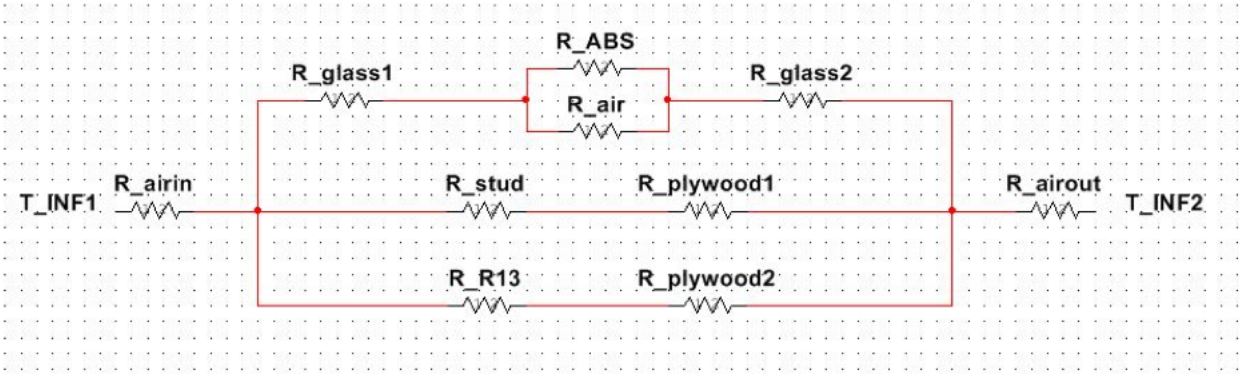

Figure 24 shows the resistance diagram for the wall without aerogel (Curtesy of Kian Cook ME '18).

Thermal resistance for convection at $R_{\_airin}$, $R_{\_airout}$, and $R_{\_air}$ is given by equation 4 where h_{air} is approximated as 5 W/m^2K. On the other hand, the conductive thermal resistance through the wall assembly is described by equation 5 where k is the thermal conductivity of the material, A is the area perpendicular to the flow of heat, and L is Length. Values used in computing resistances can be found in Appendix D.

$$R_{conv} = \frac{1}{hA} \tag{4}$$

$$R_{cond} = \frac{L}{kA} \tag{5}$$

The resulting resistances can be summed in series and parallel yielding R_{tot}. The total thermal resistance of the aerogel wall, $R_{tot\text{-}aero}$, was found to be 5.0 K/W while the total thermal resistance of the conventional wall, $R_{tot\text{-}conven,}$ was 4.03 K/W. Incorporating each into equation 3 returns a heat transfer rate of 14.0 W and 17.4 W for the aerogel and non-aerogel walls respectively, indicating a 19.5% decrease in heat loss.

5.3: Computer Model

While the 1D model was a useful tool in estimating the enhanced performance of an aerogel supplemented building envelope further analysis must be conducted in order to validate the results. Thermal modeling was conducted using Solidworks Thermal Simulation (which uses a finite element method) to corroborate the results obtained mathematically.

First, a three-dimensional model of a single wall complete with a window, studs, and insulation was created in Solidworks. Figure 25 shows the model used in the thermal simulation.

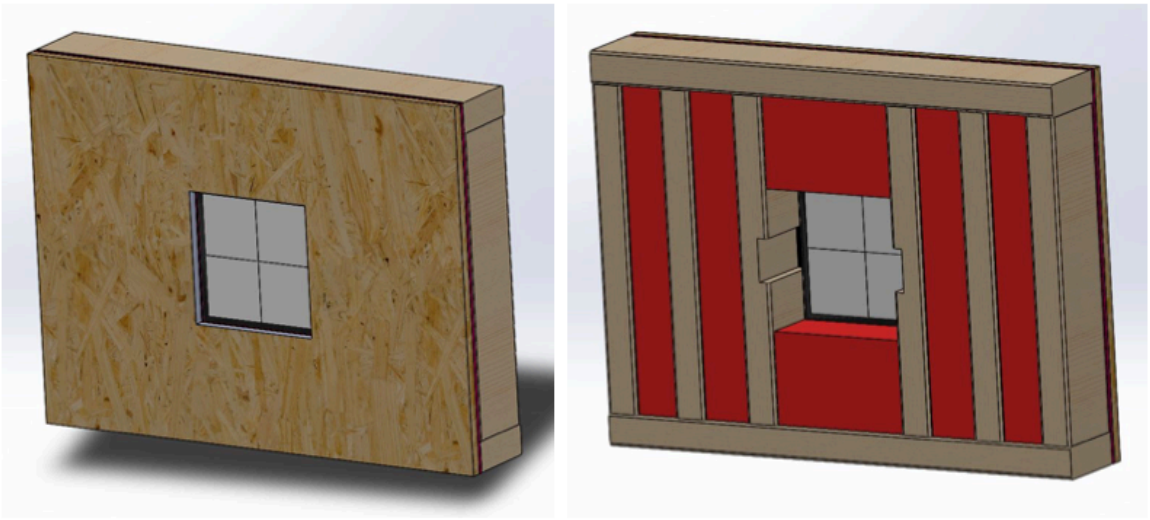

Figure 25 shows the front (left) and back (right) of the model used in the Solidworks Simulation.

The materials were assigned material properties. The thermal properties and layer thicknesses are shown below in Table 9.

Table 9 displays the material properties used in the Solidworks simulation.

Material	**Thickness (m)**	**Density ($\frac{kg}{m^3}$)**	**Thermal Conductivity ($\frac{W}{mK}$)**
Glass	1.5875 E-3	2530	0.935
ABS Plastic	1.27 E-2	1060	0.180
Plywood	1.27 E-2	600	0.130
2 x 4 Stud	8.89 E-2	400	0.140
R-13 Insulation	7.62 E-2	12.1	0.035
Aerogel Monolith	1.27 E-2	100	0.0225 [11]
Aspen Spaceloft	5.0 E-3	150	0.015 [13]

The model was constructed as a combination of a wall assembly and a separate window assembly. Solidworks models of the window assemblies with aerogel components is shown in Figure 26.

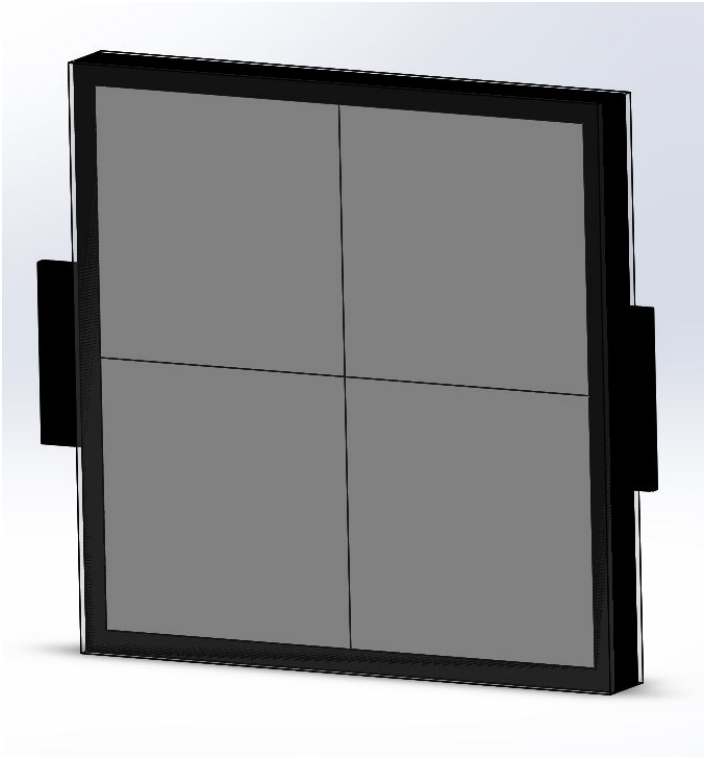

Figure 26 shows the Solidworks model of the window assembly with aerogel inserts.

The interior and exterior of the building as well as the inside of the doubles paned window experienced convective heat transfer with air having a heat transfer coefficient of 5 W/m^2K. The inner membrane was considered to be at room temperature, 21℃. The outside of the wall was exposed to air at 0℃. The model and applied boundary conditions can be seen in Figure 27.

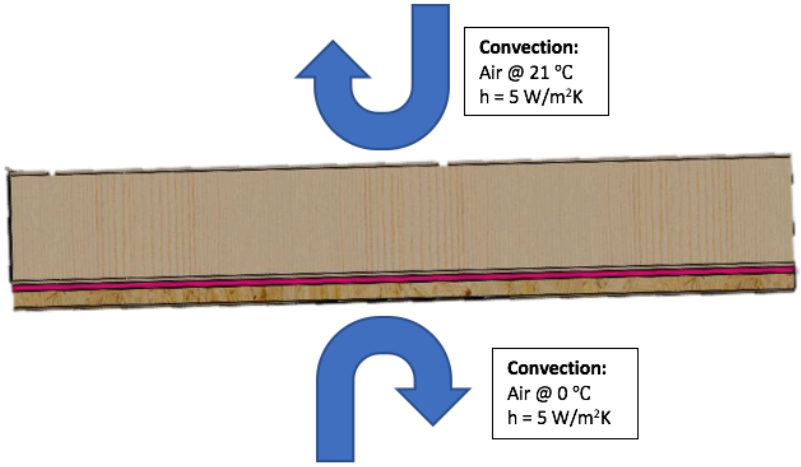

Figure 27 shows the thermal loads applied to the Solidworks model.

Two steady state simulations were conducted, the first contained a conventional, double-paned glass window with fiberglass insulation. The second model was run with an aerogel window assembly as well as 5 mm thick aerogel strips applied to the exterior of the studs. The simulation was run and the temperature gradient results for the conventional wall and aerogel wall are shown in Figure 28 and Figure 29 respectively.

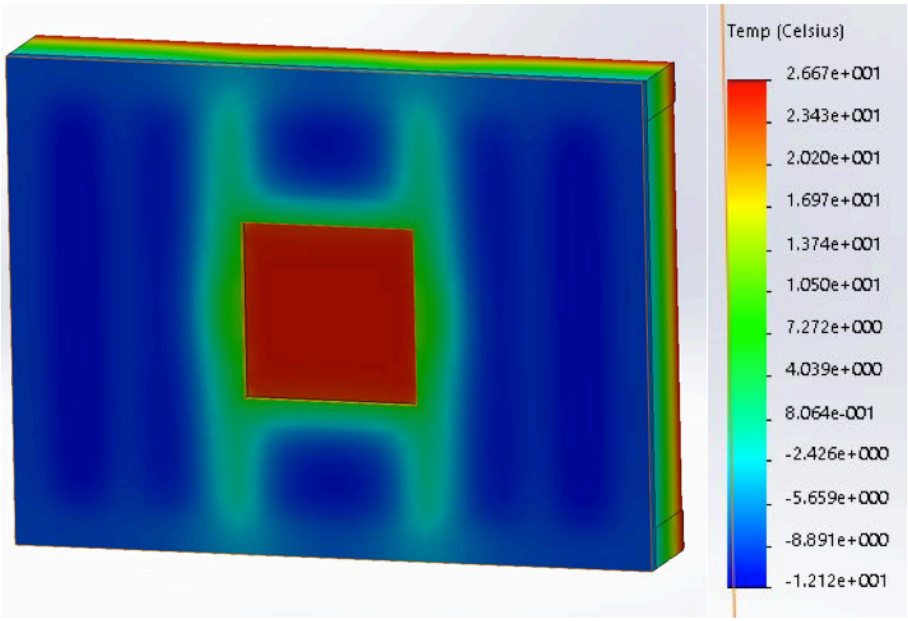

Figure 28 shows the thermal simulation results for the conventional wall assembly.

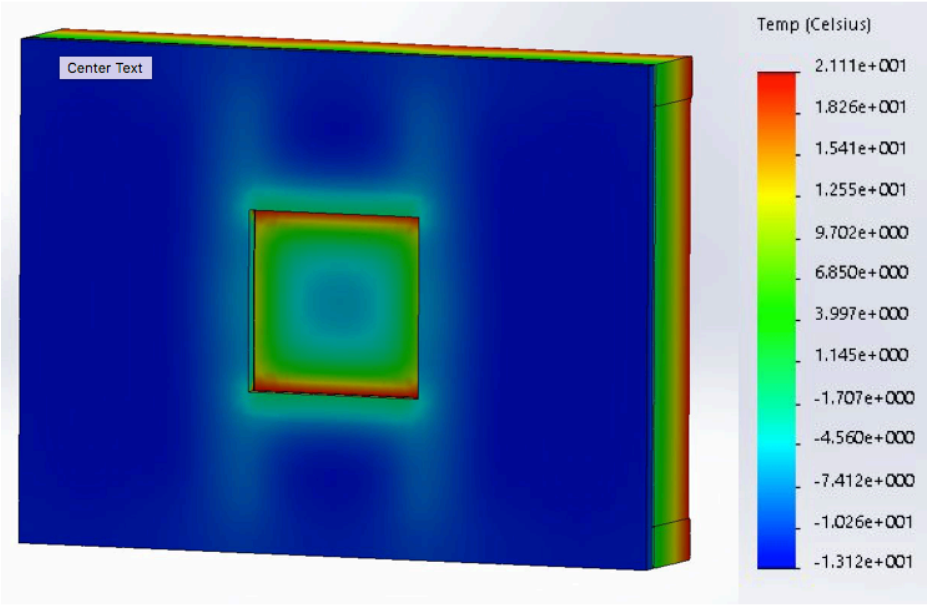

Figure 29 shows the thermal simulation results for the aerogel assembly.

The conventional window assembly proved to be a poor thermal barrier. The vertical lines framing the windows are thermal breaks; areas of warmer temperature indicating higher heat transfer through the wooden studs. Furthermore, the window shows solid red indicating a significant amount of heat loss through the double paned glass. The aerogel wall assembly is a clear improvement. The solid blue walls and green window indicate notably less heat loss through the studs and aerogel insulated window. The total heat power was found to be 12.49 W for the aerogel assembly and 18.47 W for the non-aerogel assembly, indicating a 32.4% decrease in heat loss. This is nearly 10% more than predicted via the 1D model.

5.4: Construction

While theoretical and simulated results are important in predicting the performance of an aerogel wall assembly it is important to confirm these predictions experimentally. A scaled down model home was constructed and outfitted with a heat source. Thermal images of the outside of the home were taken in order to study heat transfer through different parts of the building envelope.

The structures floor was constructed of 24 x 24 x 0.5-inch plywood square onto which 2 x 4-inch studs were attached via 1 5/8-inch drywall screws. Figure 30 shows the floor and stud assembly.

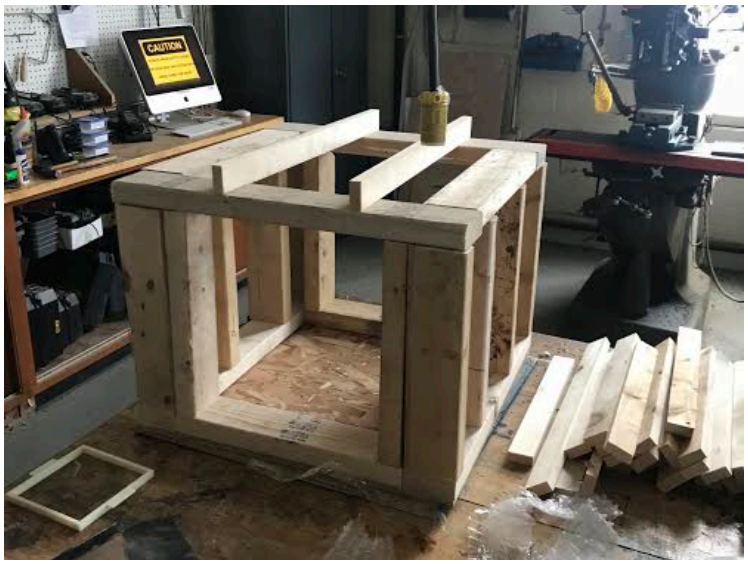

Figure 30 shows the 24 x 24-inch base and 18-inch tall wall studs.

Spaceloft strips were applied via wood glue to the exterior of the studs on two of the walls as seen in Figure 31.

Figure 31 shows the aerogel strips applied to the exterior of the studs.

The walls were 18 inches tall and sheathed with 0.5-inch-thick plywood. The roof, also composed of 0.5-inch-thick plywood, came to a peak at 31 inches. 6.5 x 6.5-inch holes were cut in two opposing walls to allow windows supplied by Kian Cook (ME ’18) to be mounted. Figure 32 shows the completed roof as well as the rough opening for one of the windows.

Figure 32 shows the installation of the roof and the rough opening for the window assembly.

While the roof was still open a hole was drilled through the center of the floor to allow the cord for a light fixture to be fed through. The model was equipped with a 100 W incandescent lightbulb to act as a heat source. R-13 faced wall insulation was installed in the bays within studs to ensure a sound thermal envelope. Caulking was used to seal any joints or holes in the plywood and prevent airflow into or out of the house creating a sound thermal envelope. Figure 33 displays the heat source, wall insulation, and caulking used to weatherproof the model.

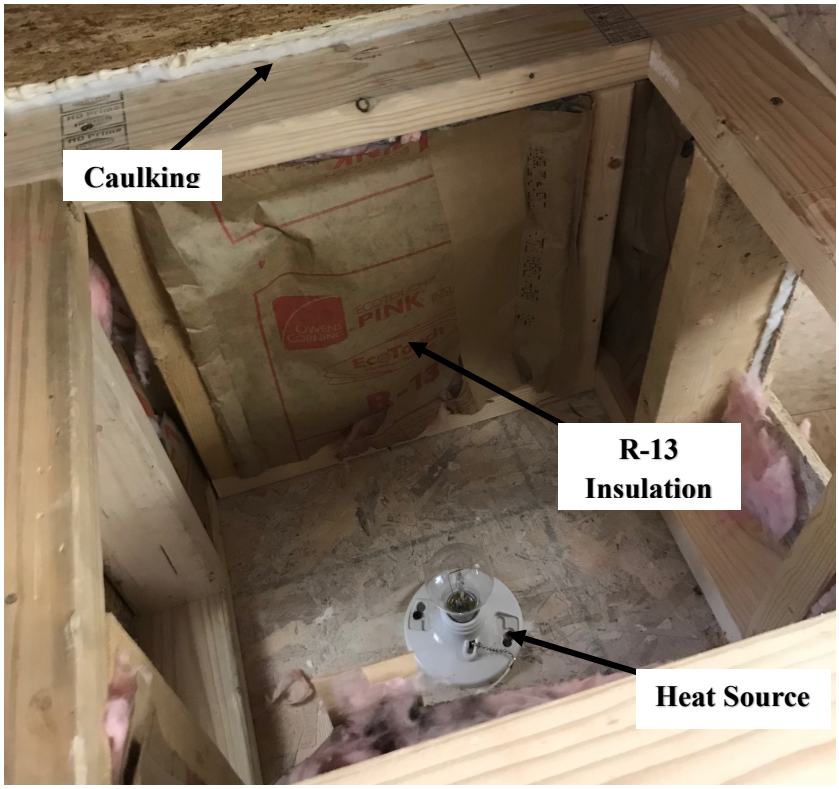

Figure 33 displays the installed heat source and insulation.

The windows consist of an ABS plastic 3D printed frame onto which two panes of glass were mounted using a silicone adhesive. One of the window assemblies was outfitted with four 3 x 3 x 0.5-inch aerogel squares which was laser cut to size. Figure 34 shows the design of the window assemblies.

Figure 34 shows the aerogel window assembly supplied by Kian Cook (ME '18).

The windows were mounted in their rough openings and weatherproofing silicone was used to attach them and ensure an airtight seal. A small hole was drilled into a wall and thermocouples were fed through in order to take temperature measurements at strategic locations. Table 10 gives the thermocouple locations and Figure 35 shows a window installation as well as the thermocouples.

Table 10 displays the location of the thermocouples.

Thermocouple	**Location**
1	Inside aerogel window
2	Inside normal window
3	Inside aerogel stud
4	Inside normal stud
5	Light bulb base
6	Hanging from rafters – ambient temperature

Figure 35 shows the thermocouple ends (left) and an installed window assembly (left).

Finally, for reasons of convenience waterproof window flashing as opposed to shingles were applied to act as roofing and a coat of paint was applied to the exterior of the house as seen in Figure 36.

Figure 36 shows the completed model home.

The model was placed in a freezer kept at 4℃, the heat source was plugged in, and it was left for four hours in order for it to reach steady state. After four hours, three readings were taken for each interior thermocouple as well as at additional thermocouples applied at complimentary locations on the exterior of the building. The results were averaged and displayed in Table 11, the temperature readings can be found in their entirety in Appendix E.

Table 11 shows the temperatures at each of the thermocouples.

Thermocouple	Location	Inside Temperature (℃)	Outside Temperature (℃)
1	aerogel window	43.17	12.44
2	normal window	41.39	16.50
3	aerogel stud	50.76	9.22
4	normal stud	47.15	9.61
5	Light bulb base	50.39	-------
6	Ambient temp.	51.67	7.33

Both the aerogel window and the aerogel stud had higher recorded interior temperatures and lower exterior temperatures than their conventional counterparts. The larger the difference between interior and exterior temperatures the more effective the thermal barrier. The aerogel window exhibited a temperature difference of 30.73℃ while the normal, double paned window had a temperature difference of 24.89℃. Similarly, the stud with aerogel sheathing displayed a temperature difference between interior and exterior measurements of 41.54℃ while the conventional stud assembly had a difference of only 37.54℃. This indicates less heat loss to the ambient through the aerogel components than through the typical installations.

Finally, a Flir C3 thermal imaging device was used to take infrared images of the exterior of the home. Figure 37 consists of thermal images of the walls with and without aerogel strips on the studs while Figure 38 shows thermal images of the walls containing window assemblies.

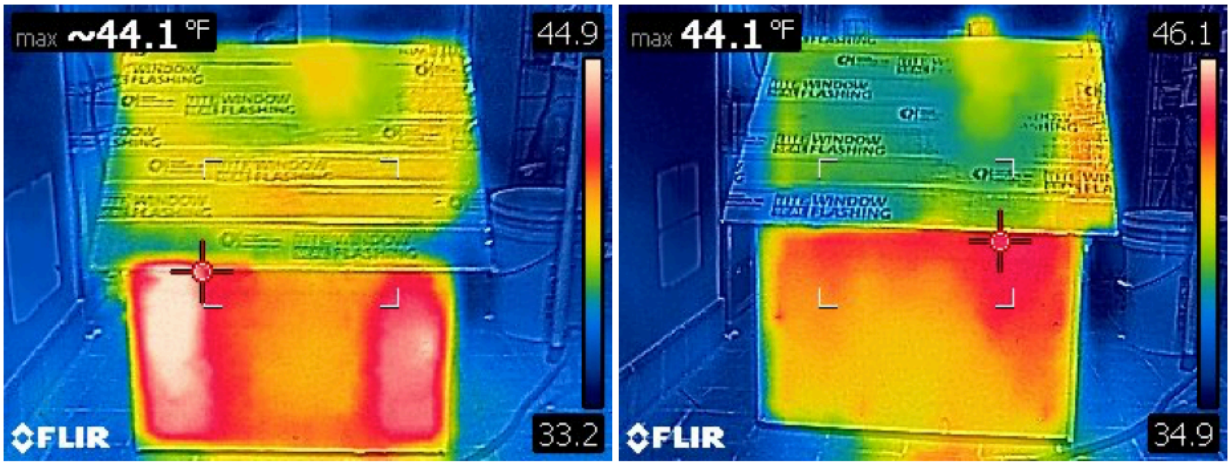

Figure 37 shows thermal images of the walls without (left) and with (right) aerogel strips applied to the studs.

Figure 38 displays thermal images of the window assemblies without (left) and with (right) aerogel.

In both situations the amount of heat lost is abated by the application of aerogel products. The thermal image of the wall without aerogel has two distinct red stripes at the location of the studs. This indicates higher temperatures thus increased heat loss in those locations. With aerogel strips applied there are no longer two distinct stripes meaning the aerogel insulation prevented a significant amount of heat loss. Likewise, the thermal image of the double pane window glows a bright red and reaches temperatures of up to 54.8 °F indicating a large amount of heat is escaping through the glazing. The aerogel window shows as a light orange color indicating its thermal properties are similar to those of the insulated walls, a significant improvement over the glass window.

Chapter 6 - Discussion

The bench tests, mathematical model, thermal simulation, and experimental results all distinctly show the effectiveness of aerogel products in preventing heat loss through a building envelope. The mathematical model and the thermal simulation predict that through the use of an aerogel window as well as aerogel insulation applied to the studs 3.37 W and 5.97 W less energy will be transmitted through a single wall of the model home. Multiplying this by a factor of four to account for each wall and considering the model is roughly 1/20 the size of a normal home, aerogel products could result in 1178 to 2086 kW-hr of energy savings per year when applied to a house assuming a heating season of October through March [27]. According to the US Department of Labor, New York City residents payed 20 cents per kilowatt hour of energy in 2017 [28]. This means that the use of aerogel insulation and windows could potentially save a homeowner between 236 and 417 dollars annually. Additionally, in New York State producing 1 kW-hr of electricity releases roughly 0.41 kilograms of CO_2 into the atmosphere [29]. Applying aerogel products to a typical residential home would result in 483 to 855 fewer kilograms of carbon dioxide being released into the atmosphere each heating season.

However, there is a significant amount of uncertainty and potential error involved in this testing. To begin, companies such as Aspen Aerogels are known to disperse microfibers such as carbon filaments throughout their blankets in order to prevent sintering, increase durability, and reduce dusting. The introduction of these microfibers improves thermal performance of the blankets at significantly higher temperature. Furthermore, the composition of Aspen's products is strictly guarded proprietary information. The lack of information about the contents of Aspen's spaceloft product as well as the absence of microfibers means a direct comparison between Spaceloft and the Union College RSCE blanket cannot reasonably be drawn.

Additionally, there were difficulties in measuring the thermal conductivities of each sample to within an acceptable degree of uncertainty. The transient plane source, or hot disk method of measuring thermal conductivities relies on the assumption of an infinite medium, a negligible heat capacity of the sensor, and a homogenous sample surface. In reality the sample is not an infinite medium and there may be an appreciable amount of heat lost to the ambient skewing the results. It is also necessary to delete the first few seconds of measured data in order to account for the influence of the insulating layers of the sensor but for materials with a low heat capacity that might not be enough to negate the influence of the sensor properties [30]. Finally, the surface of each sample was non-homogenous, consisting of a smattering of

fibrous materials and solid aerogel. This resulted in a large degree of variance between measurements that was dependent on sensor placement.

Another possible area for concern was in conducting the UL-94 burn test. To start, combustion and glow times were recorded via a stopwatch. With such short burn times it can be certain that a significant amount of human error was introduced. Thompson *et al.* reports that an individual's mean reaction time to visual stimuli is between 180 and 200 ms [31]. This could result in between 5 and 15% error in combustion and glow time measurements. Furthermore, the distance between the bottom of the sample and the blowtorch as well as the orientation of the blowtorch nozzle was not kept constant due to special constraints which could account for some variation between samples.

In constructing the mathematical model and Soldiworks simulation a number of assumptions were made which had direct ramifications on the results of each. In order to simplify mathematical calculations, only conduction and convection were considered, ignoring the effects of radiation and contact resistance. According to the Canadian Department of Natural Resources radiation accounts for roughly 10% of the heat loss through a home, mostly through windows [32]. Heat transfer across a joint is complex as contact resistance is a function of the geometry of the contacting solids, gap thickness, the type of interstitial fluid, and the yield pressure of the contacting bodies. Failing to account for both radiation and contact resistance introduced a great deal of error to the analytical results.

Furthermore, all materials were assumed to be homogenous with constant material properties, and all seams and gaps were considered airtight without need for caulking. Each of these assumptions had significant implications on the validity of the results. There is significant room for error in the construction of a home. Organic materials such as wood are non-homogenous and display a wide range of material properties depending on the temperature they are exposed to. The inconsistent nature of wood and human error lead to unavoidable gaps and cracks throughout the building envelope. One such instance can be seen in the top left of the aerogel window installation in Figure 38 (left) which glows bright white due to warm air escaping through a gap. Another such occurrence is seen in Figure 37 (right) where a large red area of increased heat transfer is seen due to hot air escaping from under the roof.

Finally, the analytical solutions assumed a constant interior surface temperature of 21°C and exterior temperature of 0°C, no heat loss through the roof or floor, and a constant heat transfer coefficient of air, h_{air}, of 5 W/m^2K. The assumption of constant interior and exterior surface temperatures is proven false experimentally as shown in Table 11 which shows values at several points inside and outside of the

model home. Likewise, the three temperature readings at each thermocouple location trended downward indicating that the building had potentially not yet reached steady state at the time of measurement. Jesse Brooks reports that a building's roof accounts for roughly 33% of heat loss in the winter and 60% of heat gain in the summer [33]. By ignoring heat transfer through the roof and floor a significant amount of the overall heat transfer into and out of the home is ignored. In order to check the approximation of the heat transfer coefficient of air the Nusselt number was found using a correlation for heat transfer in vertical rectangular channels. From the Nusselt number the heat transfer coefficient of air within the double paned window was found to be 3.43 W/m^2K indicating our assumption was within reason. Calculations for the heat transfer coefficient of air within the double paned window can be found in their entirety in Appendix F.

One final factor to be considered is the cost of implementing silica aerogel insulation on a normal home. This study will look at the additional costs accrued by applying 5 mm thick Spaceloft to the exterior of all wall studs. This study will not look at aerogel windows as reliable cost estimates could not yet be found. The amount of aerogel blanket needed was found by multiplying the surface area of studs in the mathematical model by four to account for each of the walls and then by a factor of 20 as our model was roughly 1/20 the size of a normal home. Aspen aerogels sells Spaceloft at a cost of $180 for 8 ft^2, or $22.50 per square foot. Multiplying the area of studs to be covered by the cost per square foot yields a total cost to outfit a home of $2587.50 barring the cost of labor and waste material. A consumer would have to weigh the benefits of a high initial cost to the potential for savings on heating and cooling bills when pursuing this path.

Chapter 7 - Conclusion

While great strides will continue to be made in the transition toward using renewable energies, retrofitting existing buildings with more effective insulation is an immediate option to abate energy usage and greenhouse gas emissions. This research venture was successful in that an aerogel blanket was fabricated using the Union College Rapid Supercritical Extraction (RSCE) method. Additionally, this aerogel displayed thermal characteristics similar to blankets currently available for purchase. Future testing should be done to better understand the relationship between content aerogel and blanket thermal conductivity. If this method of manufacturing aerogel blankets could effectively be scaled up it has the potential to reduce the time required to produce these aerogel products thereby reducing their cost and increasing their market presence. Furthermore, Solidworks and mathematical models were produced and confirmed that an appreciable amount of energy is to be saved by implementing aerogel windows and insulation. Finally, a mock home was constructed as realistically as possible complete with a heat source. This model will prove to be useful in conducting experimental tests with various aerogel window configurations as well as novel aerogel insulations which have yet to be developed.

Although the application of aerogel strips and windows effectively decreased heat lost through the studs and window assemblies, a number of steps must be taken before they can effectively be scaled up and mass-produced. Currently aerogel products are cost prohibitive and as such do not enjoy widespread use by contractors. In order to become commonplace measures must be taken to increase production rates and reduce costs. Furthermore, a system to quickly and easily apply the strips to the exterior of studs must be devised. Moreover, the Spaceloft samples produced a significant amount of dust when being handled. Steps must be taken to ensure the safety of workers who will be working with aerogel products as inhalation can be harmful. The final step in promoting widespread use would be passing legislation to promote the use of aerogel or similar insulation in the form of tax incentives or new building codes. This legislation could target buildings which are particularly at risk of losing energy through thermal breaks such as large, steel framed, climate-controlled buildings in colder climates.

Future improvements on this research could focus on eliminating error, improving manufacturability, and optimizing for cost. With much of the heat in a building being lost through the windows and ceiling work could be done to produce a model which determines energy savings when aerogel products are applied to all aspects of the thermal barrier as opposed to just the studs. If the RSCE method could be reproduced on a significantly larger scale aerogel insulation could be fabricated at much higher rates which would have the potential of driving prices down and increasing use and availability.

Acknowledgements

I would like to thank all those who have made significant contributions to the success of my project. I would like to thank Paul Tompkins for helping me come up with a mold design and taking the time to manufacture it. Stan Gorski and Rhonda Becker were essential in helping me acquire the necessary equipment to fabricating the aerogel blanket and completing the associated tests. I am grateful for the student research grant awarded to me by Union College which allowed me to purchase all of the necessary materials. I want to thank my parents, in particular my Father who took time out of his weekend to provide his construction expertise and help the model home to come to fruition. I would like to thank all of the aerogel students and professors who provided valuable insight and helped with many aspects of this project. Special thanks goes to Kian Cook, his tireless work on this project was an essential factor in us reaching all of our goals. Finally, thank you Professor Ann Anderson for providing me the opportunity to work in such a wonderful environment and devoting so much of her time and energy to mentoring me through this project.

Works Cited

[1] J. R. Hansen, R. Ruedy, M. Sato and K. Lo, "Global Surface Temperature Change," 2010.

[2] R. Pachauri and A. Reisinger, "Climate Change 2007," Geneva, 2007.

[3] D. Wuebbles, D. Fahey and K. Hibbard, "Climate Science Special Report," U.S. Global Change Research Program, 2017.

[4] Climate Central, "Climate Central," 19 April 2017. [Online]. Available: http://www.climatecentral.org/gallery/graphics/co2-and-rising-global-temperatures. [Accessed 10 October 2017].

[5] REN21, "Global Status Report," REN21, Paris, 2017.

[6] U.S. Energy Information Administration, "Anual Enegy Review," 2016.

[7] U.S. Energy Information Administration, "Monthly Energy Review April 2017," 2017.

[8] McKinsey & Company, "Pathways to Low Carbon Economy - Version 2 of the Global Greenhouse Gas Abatement Cost Curve," 2009.

[9] A. Lyons, Materials for Architects and Builders, vol. 4, Burlington, MA: Butterworth-Heinemann, 2010.

[10] H. Simmler, U. Heinemann, K. Kumaran, D. Quenard, K. Noller and M. Tenpierik, "Vacuum Insulation Panels - Study on VIP-components and Panels for Service Life Prediction of VIP in Building Applications (Subtask A)," 2015.

[11] A. M. Anderson and M. K. Carroll, "Hydrophobic Silica Aerogels: Review of Synthesis, Properties and Applications," Schenectady, 2011.

[12] E. Cruce, P. Cruce, C. Wood and S. Riffat, "Toward aerogel based thermal superinsulation in buildings: A comprehensive review," *Renewable and Sustainable Energy Reviews,* vol. 34, pp. 273-299, June 2014.

[13] Aspen Aerogel, "Spaceloft Data Sheet," Aspen Aerogel, Northborough, 2016.

[14] M. K. Carroll, A. M. Anderson and C. A. Gorka, "Preparing Silica Aerogel Monoliths via a Rapid Supercritical Extraction Method," Journal of Visualized Experiments, Schenectady, 2014.

[15] G. Brady, "Inrared New England," [Online]. Available: http://www.infrarednewengland.com. [Accessed 17 October 2017].

[16] J. Kosney, T. Petrie, D. Yarbrough, P. Childs, A. M. Syed and C. Blair, "Nano-Scale Insulation at Work: Thermal Performance of Thermally Bridged Wood and Steel Structures Insulated with Local Aerogel Insulation," Northborough, 2007.

[17] KC Spray Foam, "KC Spray Fooam & Coatings LLC," 08 October 2013. [Online]. Available: https://kcsprayfoam.com/r-value-alone-doesnt-matter/rvaluehotbox2/. [Accessed 09 November 2017].

[18] A. Vimmrová and . J. Výborný, "Materials and Testing Methods," in *Building Materials 10*, Prague, Vydavatelství ČVUT, 2001, p. 90.

[19] Netzsch, *Guarded Hot Plate - GHP,* Wittelsbacherstraße: NETZSCH-Gerätebau.

[20] J. Ventrella, "Thermal Conductivity of TMOS Aerogels Under Vacuum and in the Presence of Various Gases," Schenectady, 2015.

[21] T. Log and S. Gustafsson, "Transient Plane Source (TPS) Technique for Measuring Thermal Transport Properties of Building Materials," *Fire and Materials,* vol. 19, pp. 43-49, 1995.

[22] V. B. Apte, Flammability Testing of Materials Used in Construction, Transport, and Mining, Cambridge: Woodhead Publishing Limited, 2006.

[23] R. Baetens, B. Jelle Petter and A. Gustavsen, "Aerogel insulation for building applications: A state-of-the-art review," *Energy and Buildings,* vol. 43, no. 4, pp. 761-769, April 2011.

[24] H. Schmidt, "Scaling of Fire Test Results in Rigid Polyurethane Foams," 2010.

[25] Boedeker Plastics Inc., "Boedeker," 2017. [Online]. Available: http://www.boedeker.com/bpi-ul94.htm. [Accessed 10 November 2017].

[26] Department of Energy, "Insulation Fact Sheet," Oak Ridge National Laboratory, Oak Ridge, 2008.

[27] E. M. Division, "Mass. Projected Household Heating Costs," 2017. [Online]. Available: https://www.mass.gov/service-details/mass-projected-household-heating-costs. [Accessed 10 March 2018].

[28] B. o. L. Statistics, "Average Energy Prices, New York-Northern New Jersey-Long Island– November 2017," U.S. Department of Labor, 2017.

[29] U. E. I. Administration, "How much carbon dioxide is produced per kilowatthour when generating electricity with fossil fuels?," Washington D.C. , 2017.

[30] S. Gustafsson, "Transient plane source techniques for thermal conductivity and thermal diffusivity measurements of solid materials," *Review of Scientific Instruments,* vol. 65, pp. 797-804, 1991.

[31] P. Thompson , J. Colebatch , P. Brown and J. Rothwell, "Voluntary stimulus-sensitive jerks and jumps mimicking myoclonus or pathological startle syndromes.," *Mov Disorder,* vol. 7, no. 3, pp. 257-262, 1992.

[32] G. o. Canada, "Keeping the Heat in - Chapter 2: How your House Works," 23 January 2017. [Online]. Available: https://www.nrcan.gc.ca/energy/efficiency/housing/home-improvements/keeping-the-heat-in/how-your-house-works/15630. [Accessed 11 March 2018].

[33] J. Brooks, "Insulate Your Home for Comfort and Savings," University of Kentucky College of Agricultural Engineering, Lexington, 1980.

Appendix A: Solidworks Model Of The Mold

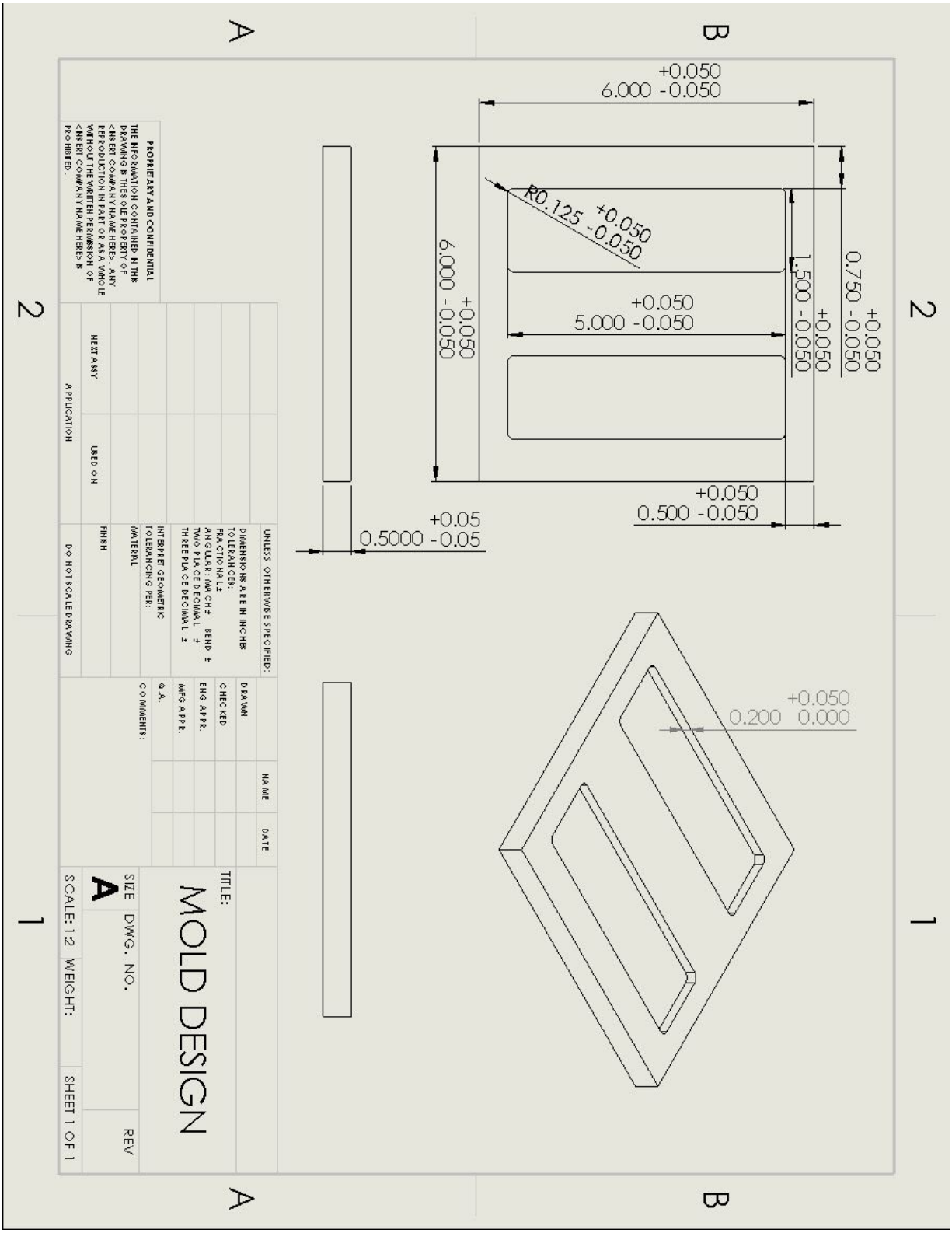

Appendix B: Record of All Samples Fabricated

Sample Number: 1-1 & 1-2 **Date: January 21, 2018**

Table 12: Hot press parameters for sample 1-1 & 1-2.

Step	Temp. (F)	Rate (F/min)	Force (kips)	Rate (kips/min)	Time
1	90	200	45	600	30
2	550	3	45	600	55
3	550	200	1	1	15
4	90	4	1	1	15

Table 13: Recipe used to create sample 1-1 & 1-2

Amount Desired	100 mL
TMOS	21.49 mL
Methanol	69.09 mL
Water	8.70 mL
1.5 M Ammonia	716.48 μL

Content	Sample 1-1	Sample 1-2
Rock Wool (g)	-------	-------
Final Weight (g)	3.3663	3.7840
Percent Aerogel (%)	(?)	(?)

Table 15: Thermal conductivity parameters & results for sample 1-1.

Run Number	Power (W)	Time (s)	k (W/mK)
1	0.05	50	0.04323
2	0.02	50	0.04354
3	0.02	100	0.04605
4	0.02	100	0.04684
5	0.02	50	0.04530

Table 14: Thermal conductivity parameters & results for sample 1-2.

Run Number	Power (W)	Time (s)	k (W/mK)
1	0.02	100	0.04751
2	0.02	100	0.04740
3	0.02	110	0.04661
4	0.02	100	0.04794
5	0.02	100	0.04630

Notes:

- Stainless steel gasket material

Sample Number: 2-1 & 2-2 **Date: January 25, 2018**

Table 16: Hot press parameters for sample 2-1 & 2-2.

Step	Temp. (F)	Rate (F/min)	Force (kips)	Rate (kips/min)	Time
1	90	200	45	600	30
2	550	3	45	600	55
3	550	200	1	1	15
4	90	2	1	1	15

Table 17: Recipe used to create sample 2-1 & 2-2

Amount Desired	100 mL
TMOS	21.49 mL
Methanol	69.09 mL
Water	8.70 mL
1.5 M Ammonia	716.48 μL

Content	Sample 2-1	Sample 2-2
Quartz Felt (g)	0.4200	0.2650
Final Weight (g)	2.2415	2.3361
Percent Aerogel (%)	81.26	88.66

Table 19: Thermal conductivity parameters & results for sample 2-1.

Run Number	Power (W)	Time (s)	k (W/mK)
1	0.009	12	0.04203
2	0.009	30	0.03540
3	0.01	40	0.03652
4	0.01	40	0.03606
5	0.01	40	0.03503

Table 18: Thermal conductivity parameters & results for sample 2-2.

Run Number	Power (W)	Time (s)	k (W/mK)
1	0.009	30	0.03616
2	0.01	30	0.03364
3	0.01	40	0.04000
4	0.01	40	0.03493
5	0.01	40	0.03529

Notes:

- Stainless steel gasket material
- Stacked with another mold

Sample Number: 3-1 & 3-2 **Date: January 26, 2018**

Table 20: Hot press parameters for sample 3-1 & 3-2.

Step	Temp. (F)	Rate (F/min)	Force (kips)	Rate (kips/min)	Time
1	90	200	45	600	30
2	550	3	45	600	55
3	550	200	1	1	15
4	90	2	1	1	15

Table 21: Recipe used to create sample 3-1 & 3-2

Amount Desired	100 mL
TMOS	21.49 mL
Methanol	69.09 mL
Water	8.70 mL
1.5 M Ammonia	1433 μL

Content	Sample 3-1	Sample 3-2
Quartz Felt (g)	0.3700	0.4461
Final Weight (g)	2.6371	2.4916
Percent Aerogel (%)	85.97	82.10

Table 23: Thermal conductivity parameters & results for sample 3-1.

Run Number	Power (W)	Time (s)	k (W/mK)
1	0.01	40	0.03291
2	0.01	40	0.02979
3	0.01	50	0.03095
4	0.01	50	0.03012
5	0.01	50	0.03041

Table 22: Thermal conductivity parameters & results for sample 3-2.

Run Number	Power (W)	Time (s)	k (W/mK)
1	0.01	40	0.03127
2	0.01	50	0.03117
3	0.01	50	0.02946
4	0.01	50	0.03025
5	0.01	50	0.03137

Notes:

- Stainless steel gasket material
- Stacked with another mold

Sample Number: 4-1 & 4-2 **Date: January 29, 2018**

Table 24: Hot press parameters for sample 4-1 & 4-2.

Step	Temp. (F)	Rate (F/min)	Force (kips)	Rate (kips/min)	Time
1	90	200	53	600	30
2	550	3	53	600	55
3	550	200	1	1	15
4	90	6	1	1	15

Table 25: Recipe used to create sample 4-1 & 4-2

Amount Desired	100 mL
TMOS	21.49 mL
Methanol	69.09 mL
Water	8.70 mL
1.5 M Ammonia	1433 μL

Content	Sample 4-1	Sample 4-2
Quartz Felt (g)	0.1860	0.1870
Final Weight (g)	2.1902	1.6870
Percent Aerogel (%)	91.51	88.97

Table 27: Thermal conductivity parameters & results for sample 4-1.

Run Number	Power (W)	Time (s)	k (W/mK)
1	0.01	50	0.03177
2	0.01	60	0.03402
3	0.01	60	0.03243
4	0.01	60	0.03243
5	0.01	60	0.03260

Table 26: Thermal conductivity parameters & results for sample 4-2.

Run Number	Power (W)	Time (s)	k (W/mK)
1	0.01	60	0.03357
2	0.01	60	0.03231
3	0.01	60	0.03369
4	0.01	60	0.03282
5	0.01	60	0.03257

Notes:

- Stainless steel gasket material
- Stacked with another mold

Sample Number: 5-1 & 5-2 **Date: January 30, 2018**

Table 28: Hot press parameters for sample 5-1 & 5-2.

Step	Temp. (F)	Rate (F/min)	Force (kips)	Rate (kips/min)	Time
1	90	200	53	600	30
2	550	3	53	600	55
3	550	200	1	1	15
4	90	6	1	1	15

Table 29: Recipe used to create sample 5-1 & 5-2

Amount Desired	100 mL
TMOS	21.49 mL
Methanol	69.09 mL
Water	8.70 mL
1.5 M Ammonia	1433 μL

Content	Sample 5-1	Sample 5-2
Quartz Felt (g)	0.3512	0.3700
Final Weight (g)	2.3765	2.4191
Percent Aerogel (%)	85.22	84.71

Table 31: Thermal conductivity parameters & results for sample 5-1.

Run Number	Power (W)	Time (s)	k (W/mK)
1	0.01	60	0.03511
2	0.01	60	0.03495
3	0.01	60	0.03480
4	0.01	60	0.03363
5	0.01	60	0.03439

Table 30: Thermal conductivity parameters & results for sample 5-2.

Run Number	Power (W)	Time (s)	k (W/mK)
1	0.01	60	0.03226
2	0.01	60	0.03104
3	0.01	60	0.03034
4	0.01	60	0.03053
5	0.01	60	0.03235

Notes:

- Aluminum gasket material
- Stacked with another mold

Sample Number: 6-1 & 6-2 **Date: January 31, 2018**

Table 32: Hot press parameters for sample 6-1 & 6-2.

Step	Temp. (F)	Rate (F/min)	Force (kips)	Rate (kips/min)	Time
1	90	200	49	600	30
2	550	3	49	600	55
3	550	200	1	1	15
4	90	2	1	1	15

Table 33: Recipe used to create sample 2-1 & 2-2

Amount Desired	100 mL
TMOS	21.49 mL
Methanol	69.09 mL
Water	8.70 mL
1.5 M Ammonia	1433 μL

Content	Sample 6-1	Sample 6-2
Rock Wool (g)	1.5800	1.5340
Final Weight (g)	3.2407	3.4131
Percent Aerogel (%)	51.25	55.06

Table 35: Thermal conductivity parameters & results for sample 6-1.

Run Number	Power (W)	Time (s)	k (W/mK)
1	0.01	60	0.05776
2	0.01	60	0.05370
3	0.01	60	0.05499
4	0.01	60	0.05406
5	0.01	60	0.05596

Table 34: Thermal conductivity parameters & results for sample 6-2.

Run Number	Power (W)	Time (s)	k (W/mK)
1	0.01	60	0.05284
2	0.01	60	0.05136
3	0.01	60	0.05283
4	0.01	60	0.05245
5	0.01	60	0.05225

Notes:

- Stainless steel gasket material
- Stacked with another mold

Sample Number: Samples for burn test (Quartz Felt) **Date: February 26, 2018**

Table 36: Hot press parameters for quartz felt burn test samples.

Step	Temp. (F)	Rate (F/min)	Force (kips)	Rate (kips/min)	Time
1	90	200	52	600	30
2	550	3	52	600	55
3	550	200	1	1	15
4	90	6	1	1	15

Table 37: Recipe used to create sample Quartz Felt burn test samples.

Amount Desired	100 mL
TMOS	21.49 mL
Methanol	69.09 mL
Water	8.70 mL
1.5 M Ammonia	716.48 μL

Content	Sample 1	Sample 2
Quartz Felt (g)	0.4430	0.3605
Final Weight (g)	2.6000	2.4900
Percent Aerogel (%)	82.96	85.52

Sample Number: Samples for burn test (Rock Wool) **Date: February 27, 2018**

Table 38: Hot press parameters for rock wool burn test samples.

Step	Temp. (F)	Rate (F/min)	Force (kips)	Rate (kips/min)	Time
1	90	200	52	600	30
2	550	3	52	600	55
3	550	200	1	1	15
4	90	6	1	1	15

Table 39: Recipe used to create sample rock wool burn test samples.

Amount Desired	100 mL
TMOS	21.49 mL
Methanol	69.09 mL
Water	8.70 mL
1.5 M Ammonia	716.48 μL

Content	Sample 1	Sample 2
Rock Wool (g)	1.8650	1.3134
Final Weight (g)	3.8351	3.1033
Percent Aerogel (%)	51.37	57.68

Appendix C: Aspen Spaceloft Conductivity Results

Table 40: Thermal conductivity of Aspen Spaceloft.

Run Number	Power (W)	Time (s)	k (W/mK)
1	0.05	20	0.03530
2	0.05	30	0.03349
3	0.05	30	0.03349
4	0.05	25	0.03467
5	0.02	40	0.03492

Appendix D: Values Used In The Mathematical Model

Table 41: Values used in the mathematical model.

Material	Length (m)	Area (m^2)	k (W/mK)
Glass	1.5875E -3	2.7258E -2	0.935
Aerogel	1.27E -2	2.323E -2	0.0225
ABS Plastic	1.27E -2	4.032E -3	0.18
Plywood	1.27E -2	2.5145E -1	0.13
Stud	8.89E -2	1.3355E -1	0.035
R-13 Insulation	7.62E -2	1.1790E -1	0.035
Spaceloft	5E -3	1.3355E -1	0.015

Air

h = 5 W/m^2K
A = 2.78709E -1 m^2

Appendix E: Temperature Readings From Thermocouples

Appendix D contains the raw temperature readings taken from thermocouples during model house testing in freezer.

Table 42: Thermocouple temperature readings inside and outside of the model home.

Thermocouple	**Location**	**Inside Temperature (°F)**			**Outside Temperature (°C)**		
1	aerogel window	110.7	109.8	108.7	55.8	54.3	53.1
2	normal window	107.4	106.5	105.6	62.4	61.2	61.6
3	aerogel stud	124.0	123.6	122.7	49.8	48.6	47.5
4	normal stud	117.6	116.8	116.1	50.4	48.9	48.7
5	Light bulb base	124.3	122.5	121.3	------	-----	-----
6	Ambient temp.	125.6	125.2	124.2	45.1	44.8	45.7

Appendix F: Nusselt Number Calculations

$$\beta = \frac{1}{T_1}$$

$$Ra_L = \frac{g\beta\,(T_1 - T_2)L^3}{\alpha V}$$

$$\overline{Nu_L} = 0.42\left(Ra_L^{0.25}\right)Pr^{0.012}\left(\frac{H}{L}\right)^{-0.3}$$

$$\overline{Nu_L} = \frac{\bar{h}L}{k}$$